Inorg. Chem. **2008**, *47*, 3787−3800

Copper Dioxygen Adducts: Formation of Bis(μ-oxo)dicopper(III) versus (μ-1,2)Peroxodicopper(II) Complexes with Small Changes in One Pyridyl-Ligand Substituent

Debabrata Maiti,[†] Julia S. Woertink,[‡] Amy A. Narducci Sarjeant,[†] Edward I. Solomon,[‡] and Kenneth D. Karlin*[,†]

Department of Chemistry, The Johns Hopkins University, Baltimore, Maryland 21218, and Department of Chemistry, Stanford University, Stanford, California 94305

Received December 17, 2007

The preference for the formation of a particular Cu_2O_2 isomer coming from (ligand)-Cu^I/O_2 reactivity can be regulated with the steric demands of a TMPA (tris(2-pyridylmethyl)amine) derived ligand possessing 6-pyridyl substituents on one of the three donor groups of the tripodal tetradentate ligand. When this substituent is an −XHR group (X = N or C) the traditional Cu^I/O_2 adduct forms a (μ-1,2)peroxodicopper(II) species (**A**). However, when the substituent is the slightly bulkier XR_2 moiety {aryl or NR_2 (R ≠ H)}, a bis(μ-oxo)dicopper(III) structure (**C**) is favored. The reactivity of one of the bis(μ-oxo)dicopper(III) species, $[\{(6tbp)Cu^{III}\}_2(O^{2-})_2]^{2+}$ (**7-O$_2$**) (6tbp = (6-^{t}Bu-phenyl-2-pyridylmethyl)bis(2-pyridylmethyl)amine), was probed, and for the first time, exogenous toluene or ethylbenzene hydrocarbon oxygenation reactions were observed. Typical monooxygenase chemistry occurred: the benzaldehyde product includes an 18-O atom for toluene/**7-^{18}O$_2$** reactivity, and a H-atom abstraction by **7-O$_2$** is apparent from study of its reactions with ArOH substrates, as well as the determination of $k_H/k_D \approx 7$ in the toluene oxygenation (i.e., $PhCH_3$ vs $PhCD_3$ substrates). Proposed courses of reaction are presented, including the possible involvement of $PhCH_2OO^•$ and its subsequent reaction with copper(I) complex, the latter derived from dynamic solution behavior of **7-O$_2$**. External TMPA ligand exchange for copper in **7-O$_2$** and O−O bond (re)formation chemistry, along with the ability to protonate **7-O$_2$** and release of H_2O_2 indicate the presence of an equilibrium between $[\{(6tbp)Cu^{III}\}_2(O^{2-})_2]^{2+}$ (**7-O$_2$**) and a (μ-1,2)peroxodicopper(II) form.

Introduction

In coordination chemistry, especially involving the use of multidentate ligands, the nature of the metal bound chelate is critical in dictating the metal complex chemistry, including structure, spin-state (where appropriate), reactivity, etc.[1–4] The ligand properties in question include the number of donor atoms, their identity (nitrogen, oxygen, sulfur, etc.), the overall ligand charge, the chelate ring size or sizes, the overall ligand donor ability and steric interactions. With respect to research in copper−dioxygen complex fundamental chemistry, with possible relevance to metallobiochemistry, it has been well demonstrated that copper−dioxygen complex formation, structure type, physical properties, and reactivity are dictated by ligand design and ligand nature.[1,4–7]

Scheme 1

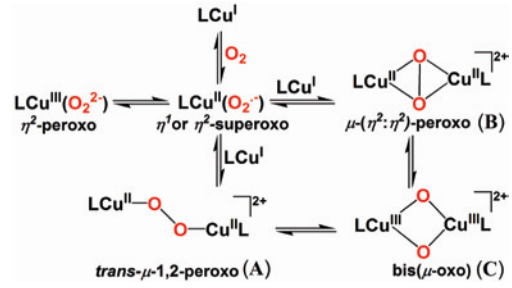

* To whom correspondence should be addressed. E-mail: karlin@jhu.edu.
[†] The Johns Hopkins University.
[‡] Stanford University.

(1) Itoh, S.; Tachi, Y. *Dalton Trans.* **2006**, 4531–4538.
(2) In *Encyclopedia of Inorganic Chemistry*, 2nd ed.; John Wiley & Sons Ltd.: New York, 2005.
(3) Lee, Y.; Karlin, K. D. Highlights of Copper Protein Active-Site Structure/Reactivity and Synthetic Model Studies. In *Concepts and Models in Bioinorganic Chemistry*; Metzler-Nolte, N., Kraatz, H.-B., Eds.; Wiley-VCH: New York, 2006; pp 363–395.
(4) Hatcher, L. Q.; Karlin, K. D. *Adv. Inorg. Chem.* **2006**, *58*, 131–184.

10.1021/ic702437c CCC: $40.75
Published on Web 04/09/2008

Chart 1

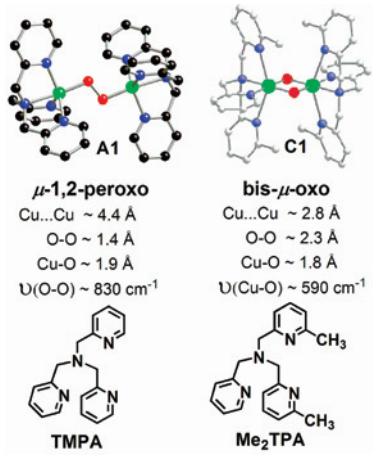

Most often, copper(I) complexes possessing tetradentate nitrogen-based ligands (alkylamino, pyridyl, imidazolyl, mixed, or others) prefer to form (μ-1,2)peroxodicopper(II) adducts (**A**), whereas tridentate ligands generally lead to dioxygen adducts described as side-on (μ-η^2:η^2)peroxo dicopper(II) complexes (**B**), and bidentate ligands most often support bis(μ-oxo)dicopper(III) complexes (**C**) (Scheme 1).[4–6] However, for a variety of tetradentate ligands, steric effects can lead to changes from structure **A** to **C**. For example, the dicopper(II) complex with TMPA (also TPA, tris(2-pyridylmethyl)amine) $[\{(TMPA)Cu^{II}\}_2(\mu-1,2\text{-}O_2^{2-})]^{2+}$ (**A1**), has an end-on structure ($\nu_{(O-O)} = 832$ ($\Delta[^{18}O_2] = -44$) cm^{-1}, $\nu_{(Cu-O)} = 561$ ($\Delta[^{18}O_2] = -26$) cm^{-1} in EtCN; $\nu_{(O-O)} = 827$ ($\Delta[^{18}O_2] = -44$) cm^{-1}, $\nu_{(Cu-O)} = 561$ ($\Delta[^{18}O_2] = -26$) cm^{-1} in Et_2O),[8,9] but with Me_2TPA ((2-pyridylmethyl)bis(6-methyl-2-pyridylmethyl)amine), Suzuki and co-workers showed that the bis-μ-oxo "isomer" $[\{(Me_2TPA)\text{-}Cu^{III}\}_2(O^{2-})_2]^{2+}$ (**C1**) ($\nu_{(Cu-O)} = 590$ ($\Delta[^{18}O_2] = -26$) cm^{-1}) results (Chart 1).[6,10,11] When all three pyridyl arms have 6-phenyl groups[12] or all are replaced by 2-quinolyl groups,[13] the derived copper(I) complexes are inert to dioxygen. For tridentate ligands, the nature of the solvent,[14–16] the counteranion,[17,18] and steric or electronic effects can change the structure from **B** to **C** or vice-versa, and in fact these two forms are often in equilibrium (Scheme 1).[6,19–24 25]

In this report, we focus on new pyridylalkylamine tetradentate ligands and their copper-dioxygen chemistry, varied in the nature of the substituent placed at the 6-position of only one of the pyridyl arms of the parent TMPA ligand. Here, what seem to be relatively subtle steric effects lead to discrimination in the type of binuclear copper-dioxygen complex formed. Specifically, when the 6-substituent first atom X also has a hydrogen atom (Chart 2; X is a −CH−, −CHR, −NHR), only the copper−dioxygen complex form **A**, (μ-1,2)peroxodicopper(II), is generated, while if the substituent is XR_2 {aryl or NR_2 ($R \neq H$)}, then only bis(μ-oxo)dicopper(III) complexes **C** are formed. The ligand complexes compared here, including examples from the literature, are shown in Chart 2; they are divided into the two groups being discussed. For four cases, this article describes new previously uncharacterized ligand−copper(I)/O_2 reactivity, spectroscopic characterization of **A** and **C**, and reactivity studies of bis(μ-oxo)dicopper(III) complex **C** including substrate oxidation/oxygenation, ligand exchange, and bond (re)formation chemistry.

Experimental Section

Materials and Methods. Unless otherwise stated, all solvents and chemicals used were of commercially available analytical grade. Tetrahydrofuran (THF) and pentane were used after they were passed through a 60 cm long column of activated alumina (Innovative Technologies, Inc.) under argon. Preparation and handling of air-sensitive compounds were performed under an argon atmosphere using standard Schlenk techniques or in an MBraun Labmaster 130 inert atmosphere (<1 ppm O_2, <1 ppm H_2O) drybox filled with nitrogen. Deoxygenation of solvents was achieved by either repeated freeze/pump/thaw cycles or bubbling with argon for 30−45 min. Elemental analyses were performed by Desert Analytics (Tucson, AZ). ^{1}H NMR spectra were measured on a Bruker 400 MHz spectrometer. Chemical shifts were reported as δ values relative to an internal standard (Me_4Si) and the residual solvent proton peak.

(5) Quant Hatcher, L.; Karlin, K. D. *J. Biol. Inorg. Chem.* **2004**, *9*, 669–683.
(6) Mirica, L. M.; Ottenwaelder, X.; Stack, T. D. P. *Chem. Rev.* **2004**, *104*, 1013–1045.
(7) Lewis, E. A.; Tolman, W. B. *Chem. Rev.* **2004**, *104*, 1047–1076.
(8) Baldwin, M. J.; Ross, P. K.; Pate, J. E.; Tyeklár, Z.; Karlin, K. D.; Solomon, E. I. *J. Am. Chem. Soc.* **1991**, *113*, 8671–8679.
(9) Jacobson, R. R.; Tyeklár, Z.; Karlin, K. D.; Liu, S.; Zubieta, J. *J. Am. Chem. Soc.* **1988**, *110*, 3690–3692.
(10) Hayashi, H.; Fujinami, S.; Nagatomo, S.; Ogo, S.; Suzuki, M.; Uehara, A.; Watanabe, Y.; Kitagawa, T. *J. Am. Chem. Soc.* **2000**, *122*, 2124–2125.
(11) Replacement of one pyridyl arm of TMPA by the more sterically demanding quinolyl group affords a (μ-1,2) peroxodicopper(II) species, whereas two quinolyl subunits in place of pyridyl donors of TMPA produces an equilibrium mixture of (μ-1,2) peroxodicopper(II) and bis(μ-oxo)dicopper(III) species. These results are to be reported elsewhere.
(12) Chuang, C.-L.; Lim, K.; Chen, Q.; Zubieta, J.; Canary, J. W. *Inorg. Chem.* **1995**, *34*, 2562–2568.
(13) Karlin, K. D.; Wei, N.; Jung, B.; Kaderli, S.; Niklaus, P.; Zuberbühler, A. D. *J. Am. Chem. Soc.* **1993**, *115*, 9506–9514.
(14) Liang, H. C.; Henson, M. J.; Hatcher, L. Q.; Vance, M. A.; Zhang, C. X.; Lahti, D.; Kaderli, S.; Sommer, R. D.; Rheingold, A. L.; Zuberbuhler, A. D.; Solomon, E. I.; Karlin, K. D. *Inorg. Chem.* **2004**, *43*, 4115–4117.
(15) Cahoy, J.; Holland, P. L.; Tolman, W. B. *Inorg. Chem.* **1999**, *38*, 2161–2168.
(16) Mahapatra, S.; Halfen, J. A.; Wilkinson, E. C.; Pan, G.; Wang, X.; Young, J., V. G.; Cramer, C. J.; Que, J., L.; Tolman, W. B. *J. Am. Chem. Soc.* **1996**, *118*, 11555–11574.
(17) Stack, T. D. P. *Dalton Trans.* **2003**, 1881–1889.
(18) Ottenwaelder, X.; Rudd, D. J.; Corbett, M. C.; Hodgson, K. O.; Hedman, B.; Stack, T. D. P. *J. Am. Chem. Soc.* **2006**, *128*, 9268–9269.
(19) Hatcher, L. Q.; Vance, M. A.; Narducci Sarjeant, A. A.; Solomon, E. I.; Karlin, K. D. *Inorg. Chem.* **2006**, *45*, 3004–3013.
(20) Que, L., Jr.; Tolman, W. B. *Angew. Chem., Int. Ed.* **2002**, *41*, 1114–1137.
(21) Mahadevan, V.; Henson, M. J.; Solomon, E. I.; Stack, T. D. P. *J. Am. Chem. Soc.* **2000**, *122*, 10249–10250.
(22) Siegbahn, P. E. M. *J. Biol. Inorg. Chem.* **2003**, *8*, 577–585.
(23) Henson, M. J.; Vance, M. A.; Zhang, C. X.; Liang, H.-C.; Karlin, K. D.; Solomon, E. I. *J. Am. Chem. Soc.* **2003**, *125*, 5186–5192.
(24) Obias, H. V.; Lin, Y.; Murthy, N. N.; Pidcock, E.; Solomon, E. I.; Ralle, M.; Blackburn, N. J.; Neuhold, Y.-M.; Zuberbühler, A. D.; Karlin, K. D. *J. Am. Chem. Soc.* **1998**, *120*, 12960–12961.
(25) Itoh, S.; Fukuzumi, S. *Bull. Chem. Soc. Jpn.* **2002**, *75*, 2081–2095.

Chart 2

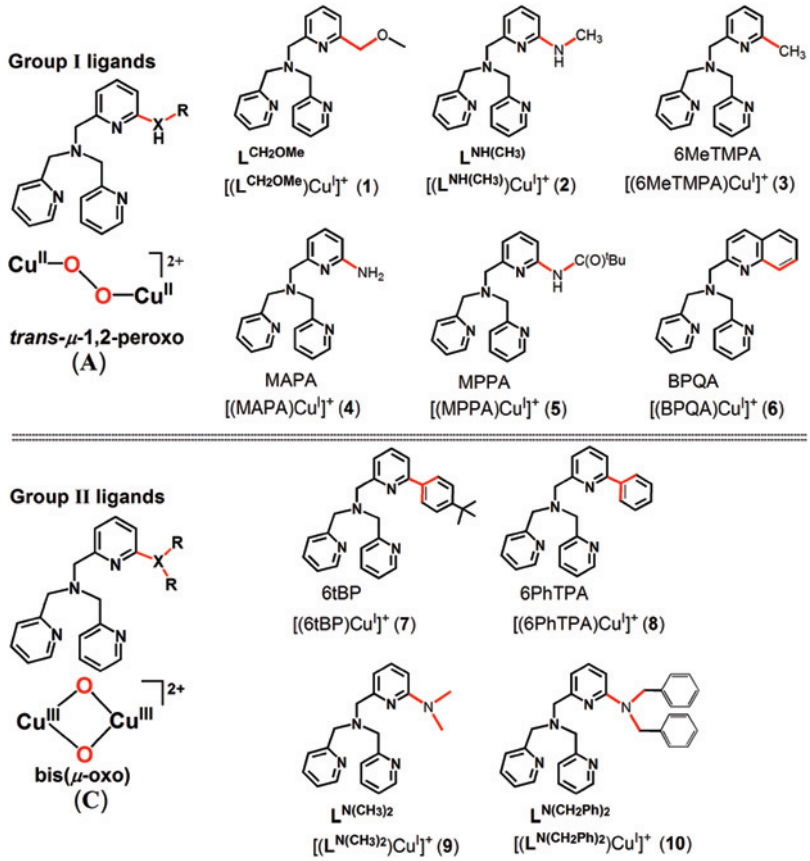

UV–vis spectra were recorded with either a Cary-50 Bio spectrophotometer equipped with a fiber optic coupler (Varian) and a fiber optic dip probe (Hellma 661.302 QX-UV 2 mm for low-temperature) or a Hewlett-Packard Model 8453A diode array spectrophotometer equipped with a two-window quartz H.S. Martin Dewar filled with cold MeOH (25 to −85 °C) maintained and controlled by a Neslab VLT-95 low temp circulator attached to the HP spectrophotometer. Spectrophotometer cells used were made by Quark Glass with column and pressure/vacuum side stopcock and 2 mm path length. Dioxygen was dried by passing through a short column of supported P_4O_{10} (Aquasorb, Mallinckrodt) and was bubbled into reaction solutions via an 18-gauge, 24 in. long stainless steel syringe needle. IR spectra were collected using a Mattson Instruments Galaxy series FT-IR (model 4030) that was controlled by the PC program WinFIRST. The copper(I) complex used for low-temperature UV–vis and all reactivity studies reported below are the $B(C_6F_5)_4^-$ salt complexes unless otherwise stated. ESI mass spectra were acquired using a Finnigan LCQDeca ion-trap mass spectrometer equipped with an electrospray ionization source (Thermo Finnigan, San Jose, CA). Samples were dissolved in CH_3OH and introduced into the instrument at a rate of 10 μL/min using a syringe pump via a silica capillary line. The heated capillary temperature was 250 °C, and the spray voltage was 5kV. X-ray diffraction was performed at the X-ray diffraction facility at the Johns Hopkins University. The X-ray intensity data were measured on an Oxford Diffraction Xcalibur3 system equipped with a graphite monochromator and an Enhance (Mo) X-ray Source (λ = 0.71073Å) operated at 2 kW power (50 kV, 40 mA) and a CCD detector. The frames were integrated with the Oxford Diffraction CrysAlisRED software package. X-band electron paramagnetic resonance (EPR) spectra were recorded on a Bruker EMX CW-EPR spectrometer controlled with a Bruker ER 041 XG microwave bridge operating at X-band (~9.472 GHz). The low-temperature experiments were carried out in THF solvent at 77 K using a $N_{2(l)}$ finger dewar.

Synthesis of $L^{N(CH_2Ph)_2}$. To BrTMPA[26] (2.4 g, 6.5 mmol) (=(6-bromo-2-pyridylmethyl)bis(2-pyridylmethyl)amine) in a pressure tube were added $(PhCH_2)_2NH.HCl$ (6.43 g, 32.5 mmol) (Aldrich), NaOH (0.78 g, 0.195 mmol), and water (15 mL). The resulting mixture was stirred and heated to 433 K for 54 h and then cooled to RT (room temperature). The resulting mixture was extracted with CH_2Cl_2 several times; the combined organic layers were dried over Na_2SO_4, and the volatile components were removed by rotary evaporation. The mixture was chromatographed on alumina (Activated Alumina, Chromatographic grade, 80–200 mesh) using 2% (progressively brought to 5%) methanol in dichloromethane as eluant. The product fraction was collected, and the solvent was removed under reduced pressure to afford the reddish-yellow oil $L^{N(CH_2Ph)_2}$ (1.95 g, 62% yield). ^1H NMR ($CDCl_3$): δ 3.71 (s, 2H, CH_2Py), 3.89 (s, 4H, $2CH_2Py$), 4.81 (s, 4H, $2CH_2Ph$) 6.33 (d, 1H), 6.76 (d, 1H), 7.08 (t, 2H), 7.21–7.35 (m, 11H), 7.52 (t, 2H), 7.63 (d, 2H), 8.49 (d, 2H).

(26) Chuang, C.-L.; dos Santos, O.; Xu, X.; Canary, J. W. *Inorg. Chem.* **1997**, *36*, 1967–1972.

^{13}C NMR ($CDCl_3$): δ 50.90, 53.44, 60.23, 77.40, 104.01, 111.45, 121.78, 122.80, 126.88, 126.97, 128.18, 128.52, 136.36, 137.77, 138.76, 140.33, 148.91, 157.26, 158.19, 160.09. ESI-MS (486.50, M + H). R_f = 0.37, alumina, 2% MeOH + CH_2Cl_2.

Reaction of $[(L^{CH_2OMe})Cu^I]^+$ (1) with O_2. The synthesis and characterization of tetradentate ligand L^{CH_2OMe} and copper(I) complex, $[L^{CH_2OMe})Cu^I]B(C_6F_5)_4$ (**1**) (Chart 2) were previously reported.[27] Crystallographically characterized $[L^{CH_2OMe})Cu^I]B(C_6F_5)_4$ (0.0049 g, 0.004 mmol) was dissolved in 3.8 mL of THF and taken in a UV–vis cuvette inside the dry box. Dioxygen was bubbled through −80 °C cold cuvette solution for 30 s with a long syringe needle. The purple product was characterized as $[\{(L^{CH_2OMe})Cu^{II}\}_2(O_2^{2-})]^{2+}$ (**1-O_2**), a μ-1,2-peroxodicopper(II) complex.

Synthesis of Copper(I) Complex $[(L^{NH(CH_3)})Cu^I]^+$ (2). The generation and characterization of tetradentate ligand $L^{NH(CH_3)}$ (Chart 2) were previously reported.[28] $L^{NH(CH_3)}$ (0.055 g, 0.172 mmol) and $[Cu^I(CH_3CN)_4]B(C_6F_5)_4$[29] (0.156 g, 0.172 mmol) were placed in a 25 mL Schlenk flask under argon. THF (3 mL) was added under argon to the mixture of solids to form a yellow solution. The resulting solution was stirred under argon for 30 min. Pentane (15 mL) was then added to the solution to precipitate a yellow solid. The supernatant was decanted, and the solid was recrystallized three times from THF/pentane under argon and dried under vacuum (1 h), giving 0.129 g of yellow powder (71% yield). ^{1}H NMR (CD_3NO_2): δ 1.76 (m, 4H, THF), 3.19 (s, 3H, CH_3), 3.59 (m, 4H, THF), 4.10 (s, 2H, CH_2), 4.24 (s, 4H, $2CH_2$), 7.0–7.8 (m, 5H), 8.1–8.8 (m, 6H). Anal. Calcd for $C_{47}H_{29}BCuF_{20}N_5O$: C, 49.78; H, 2.58; N, 6.18. Found: C, 49.50; H, 2.59; N, 5.90.

Reaction of $[(L^{NH(CH_3)})Cu^I]^+$ (2) with O_2. A THF solution (3.1 mL) of $[(L^{NH(CH_3)})Cu^I]B(C_6F_5)_4$ (**2**) (0.003 g, 0.003 mmol) was taken in a UV–vis cuvette assembly under argon and cooled to −80 °C, and an initial spectrum was recorded. Dioxygen was bubbled for 20 s through the solution using a long syringe needle, and a new spectrum recorded. Additional bubbling did not change the spectrum further.

Synthesis of Copper(I) Complex, $[(L^{N(CH_2Ph)_2})Cu^I]^+$ (10). $L^{N(CH_2Ph)_2}$ (0.050 g, 0.103 mmol) and $[Cu^I(CH_3CN)_4]B(C_6F_5)_4$[29] (0.093 g, 0.103 mmol) were placed in a 25 mL Schlenk flask under argon. THF (2 mL) was added with stirring to form a yellow solution under argon. Pentane (30 mL) was then added to the solution to precipitate a yellow solid. The supernatant was decanted, and the solid was recrystallized three times from THF/pentane. The solid obtained was washed with pentane and dried under vacuum (1 h), giving 0.097 g of yellow powder (77% yield). ^{1}H NMR (DMSO-d_6): δ 0.88 (t, 6H, $2CH_3$, C_6H_{14}), 1.27 (m, 8H, $4CH_2$, C_6H_{14}), 2.10 (s, 2H, $0.3CH_3COCH_3$), 3.36 (s, 5H, $2.5H_2O$), 3.73 (s, 2H, CH_2Py), 4.01 (s, 4H, $2CH_2Py$), 4.93 (s, 4H, $2CH_2Ph$), 6.61 (d, 1H), 6.71 (d, 1H), 7.2–7.6 (m, 15H), 7.91 (t, 2H), 8.72 (d, 2H). Anal. Calcd for $C_{62.9}H_{51.8}BCuF_{20}N_5O_{2.8}$: C, 54.87; H, 3.79; N, 5.09. Found: C, 54.80; H, 3.81; N, 4.84.

Reaction of $[(L^{N(CH_2Ph)_2})Cu^I]B(C_6F_5)_4$ (10) with O_2. Three milliliters of an acetone solution of $[(L^{N(CH_2Ph)_2})Cu^I]^+$ (**10**) (0.009 g, 0.007 mmol) was taken in a UV–vis cuvette assembly under argon which was cooled to −80 °C, and an initial spectrum was recorded. Dioxygen was bubbled for 30 s through the solution using a long syringe needle and the new spectrum recorded (see Supporting Information, Figure S1). The product was characterized as $[\{(L^{N(CH_2Ph)_2})Cu^{III}\}_2(O^{2-})_2]^{2+}$ (**10-O_2**), a bis-μ-oxo-dicopper(III) complex.

Synthesis of $[\{(L^{N(CH_2Ph)_2})Cu^{II}(Cl)\}_2]^{2+}$. $[(L^{N(CH_2Ph)_2})Cu^I]B(C_6F_5)_4$ (0.055 g, 0.044 mmol) was dissolved in THF (3.0 mL) in a 25 mL Schlenk flask. Upon removal of this flask from glovebox to the benchtop, the addition of 0.3 mL of $CHCl_3$ resulted in a green copper complex. Pentane (35 mL) was added to precipitate the copper complex. The green copper complex was further recrystallized from THF/pentane and resulted in X-ray quality crystals of $[\{(L^{N(CH_2Ph)_2})Cu^{II}(Cl)\}_2]^{2+}$ (0.042 g, 74%) (see Supporting Information, Figure S3). As seen before,[30] $CHCl_3$ is the chloride source for this complex; the copper(I) complex reacts reductively with the chlorocarbon, oxidizing copper and leading to a chloride-bound Cu(II) product. Infrared (Nujol mull): 3490 cm^{-1} (w, br, H_2O). EPR: $g_{||}$ = 2.218, $g_\perp$ = 2.042, $A_{||}$ = 182 G, $A_\perp$ = 41.5 G. Anal. Calcd for $(C_{56}H_{35}BClCuF_{20}N_5O_2)_2$: C, 51.75; H, 2.71; N, 5.39. Found: C, 51.47; H, 2.55; N, 5.09.

Reaction of $[(L^{N(CH_3)_2})Cu^I]B(C_6F_5)_4$ (9) with O_2. The synthesis and characterization of tetradentate ligand $L^{N(CH_3)_2}$ and copper(I) complex, $[(L^{N(CH_3)_2})Cu^I]B(C_6F_5)_4$ (**9**) were previously reported.[28] A 3.8 mL Et_2O solution of $[(L^{N(CH_3)_2})Cu^I]^+$ (**9**) (0.005 g, 0.005 mmol) was taken in a UV–vis cuvette assembly under argon and was cooled to −80 °C, and an initial spectrum was recorded. Dioxygen was bubbled for 30 s through the solution using a long syringe needle, and the new spectrum was recorded (see Supporting Information, Figure S2). The product was characterized as $[\{(L^{N(CH_3)_2})Cu^{III}\}_2(O^{2-})_2]^{2+}$ (**9-O_2**).

Synthesis of $[\{(6tbp)Cu^{II}(Cl)\}_2]^{2+}$. In a 25 mL Schlenk flask, $[(6tbp)Cu^I]B(C_6F_5)_4$ (0.100 g, 0.086 mmol) was dissolved in 4 mL of THF under an argon atmosphere. The resulting yellow solution was stirred at room temperature, and $CHCl_3$ (0.5 mL) was then added under argon, whereupon the solution ceased to look transparent, and its color instantly turned to green. After 2 h, 35 mL of pentane was added to precipitate the copper complex, which was recrystallized from THF/pentane. X-ray quality crystals of the dimer complex $[\{(6tbp)Cu^{II}(Cl)\}_2]^{2+}$ were obtained (see Supporting Information, Figure S3) from THF solution of the compound by layering with pentane. After they were vacuum-dried, the green crystals weighed 0.085 g (83%). Anal. Calcd for

(27) Maiti, D.; Woertink, J. S.; Vance, M. A.; Milligan, A. E.; Narducci Sarjeant, A. A.; Solomon, E. I.; Karlin, K. D. *J. Am. Chem. Soc.* **2007**, *129*, 8882–8892.
(28) Maiti, D.; Narducci Sarjeant, A. A.; Karlin, K. D. *J. Am. Chem. Soc.* **2007**, *129*, 6720–6721.
(29) Liang, H.-C.; Kim, E.; Incarvito, C. D.; Rheingold, A. L.; Karlin, K. D. *Inorg. Chem.* **2002**, *41*, 2209–2212.
(30) Lucchese, B.; Humphreys, K. J.; Lee, D.-H.; Incarvito, C. D.; Sommer, R. D.; Rheingold, A. L.; Karlin, K. D. *Inorg. Chem.* **2004**, *43*, 5987–5998.

($C_{52}H_{30}BClCuF_{20}N_4)_2$: C, 52.02; H, 2.52; N, 4.67. Found: C, 51.51; H, 2.80; N, 4.51. EPR: $g_{\|} = 2.219$, $g_{\perp} = 2.041$, $A_{\|} = 176$ G, $A_{\perp} = 37.7$ G.

Reaction of [(6tbp)Cu^{I}]B(C$_6$F$_5$)$_4$ (7) with O$_2$. Crystallographically characterized[31] [(6tbp)Cu^{I}]B(C$_6$F$_5$)$_4$ (**7**) (0.009 g, 0.008 mmol) was dissolved in 4.0 mL of Et_2O and was transferred in the UV–vis cuvette inside the MBraun drybox. Outside on the benchtop, the cuvette was cooled to −80 °C, and an initial spectrum was recorded. Dioxygen was bubbled through the solution with a long syringe needle. This results in an immediate color change from colorless to a yellowish-brown (excess dioxygen removed) EPR silent complex. The product is formulated as [{(6tbp)Cu^{III}}$_2$(O^{2-})$_2$](B(C$_6$F$_5$)$_4$)$_2$ (**7-O$_2$**), a bis-μ-oxo-dicopper(III) complex.

Reaction of [{(6tbp)Cu^{III}}$_2$(O^{2-})$_2$](B(C$_6$F$_5$)$_4$)$_2$ (7-O$_2$) with 1:1 PhCH$_3$ and PhCD$_3$. [(6tbp)Cu^{I}]B(C$_6$F$_5$)$_4$ (**7**) (0.046 g, 0.039 mmol) was dissolved in a mixture of 0.477 g of $PhCH_3$ and 0.492 g of $PhCD_3$ in the glovebox. After the mixture was cooled to −80 °C, dioxygen was bubbled through the solution for 10 s with a long needle, and [{(6tbp)Cu^{III}}$_2$(O^{2-})$_2$]$^{2+}$ (**7-O$_2$**) was formed; excess dioxygen was removed carefully via evacuation and purging with argon. After one hour, the solution was warmed to room temperature and was transferred to a 20 mL vial connected with an adaptor. The resulting solution was concentrated by careful rotary evaporation until ∼ 0.3 mL of solution remained. The copper complex was precipitated by addition of 10 mL of pentane. Further washing was carried out two more times with 15 mL of pentane, and the collective pentane washes were dried over Na_2SO_4, filtered, concentrated, and subjected to GC-MS analyses (see below, for conditions), which confirmed the formation of PhCHO and PhCDO in ∼7:1 ratio (see Supporting Information Figure S5). (Note: Authentic commercial PhCHO was used for comparison.)

Reaction of *p*-Thiocresol with [{(6tbp)Cu^{III}}$_2$(O^{2-})$_2$](B(C$_6$F$_5$)$_4$)$_2$ in Et$_2$O. [(6tbp)Cu^{I}]B(C$_6$F$_5$)$_4$ (**7**) (0.035 g, 0.030 mmol) was dissolved in a 10 mL Schlenk flask with 3 mL of Et_2O inside the glovebox. Removal of this flask from glovebox to the benchtop and cooling to −80 °C, followed by bubbling O_2 (15 s) via a long syringe needle, was carried out to generate [{(6tbp)Cu^{III}}$_2$(O^{2-})$_2$]$^{2+}$ (**7-O$_2$**). Excess dioxygen was removed carefully via evacuation and purging with argon. *p*-Thiocresol (0.005 g, 0.040 mmol) was added to the solution of [{(6tbp)Cu^{III}}$_2$(O^{2-})$_2$]$^{2+}$; the resulting mixture was bubbled with argon for 5 s to ensure thorough mixing with the substrate at −80 °C. The reaction solution was warmed up to RT after three hours, transferred to a 20 mL vial, connected with an adaptor, and concentrated by rotary evaporation until ∼0.4 mL of solution remained. This was transferred by syringe to a larger flask, and pentane (15 mL) was added. The pentane solution was decanted, and the remaining solid washed three more times with pentane (30 mL), whereupon the pentane solutions were combined and dried over Na_2SO_4. After filtration and concentration, the pentane solution was analyzed by GC and GC-MS (Figure S6, see below, for conditions) revealing the formation of *p*-tolyl disulfide (∼70% yield, GC, GC-MS, authentic commercial *p*-tolyl disulfide was used for comparison).

Reaction of Ethyl benzene with 7-O$_2$. In a 10 mL Schlenk flask, 4 mL of an ethylbenzene solution of [(6tbp)Cu^{I}]B(C$_6$F$_5$)$_4$ (0.030 g, 0.025 mmol) was prepared in the glovebox. The flask was cooled to −80 °C. O_2 was bubbled for 10 s using a long syringe needle to form [{(6tbp)Cu^{III}}$_2$(O^{2-})$_2$](B(C$_6$F$_5$)$_4$)$_2$ (excess O_2 removed). The resulting solution was warmed up to RT after 4 h, whereupon rotary evaporation concentrated the solution to ∼0.4 mL. The copper complex was precipitated out by 20 mL of pentane and was washed two more times with 30 mL of pentane. The collective pentane washes were dried over Na_2SO_4, filtered, concentrated, and subjected to GC and GC-MS analyses (see Figure S7, see below, for conditions), which confirmed the formation of $PhCOCH_3$ (authentic commercial $PhCOCH_3$ was used for comparison). After it was washed with pentane, the copper product was further purified by recrystallization from Et_2O/pentane, giving 0.026 g (yield ∼85%) of product identified as [(6tbp)$_2$Cu$^{II}_2$(OH)$_2$](B(C$_6$F$_5$)$_4$)$_2$ (**7-OH**, see Results and Discussion). The complex is EPR silent, and $\nu_{OH} = 3580$ cm^{-1} (see Supporting Information, Figure S8). Anal. Calcd for [(6tbp)$_2$Cu$^{II}_2$(OH)$_2$](B(C$_6$F$_5$)$_4$)$_2$; $C_{52}H_{31}BCuF_{20}N_4O$: C, 52.83; H, 2.64; N, 4.74. Found: C, 52.47; H, 2.68; N, 4.64.

Reaction of 7-O$_2$ with Hydroquinone. In a 100 mL Schlenk flask, an 11 mL Et_2O solution of [(6tbp)Cu^{I}]B(C$_6$F$_5$)$_4$ (**7**) (0.056 g, 0.048 mmol) was prepared in the dry box, and this was removed to the benchtop and cooled to −80 °C. Dioxygen was bubbled through the solution to form [{(6tbp)Cu^{III}}$_2$(O^{2-})$_2$](B(C$_6$F$_5$)$_4$)$_2$ (**7-O$_2$**) (excess O_2 removed). A 100 μL solution of hydroquinone (0.003 g, 0.027 mmol) was added, and the solution kept chilled for 3 h. Pentane (40 mL) was added to the resulting solution, and then removed from the resulting solid by decantation. Three additional pentane washes were carried out. The volume of the combined pentane solutions was reduced and dried over Na_2SO_4, whereupon GC and GC-MS analysis (Supporting Information Figure S9, see below, for conditions) confirmed the formation of 1,4-benzoquinone (also, compared with authentic commercial 1,4-benzoquinone) in ∼ 95% yield.

Reaction of 2,4,6-^{t}Bu$_3$-phenol with [{(6tbp)Cu^{III}}$_2$(O^{2-})$_2$](B(C$_6$F$_5$)$_4$)$_2$ (7-O$_2$). A solution of 2,4,6-^{t}Bu$_3$-phenol (0.006 g, 0.023 mmol) was prepared in 100 μL of Et_2O inside the glovebox. [(6tbp)Cu^{I}]B(C$_6$F$_5$)$_4$ (0.025 g, 0.022 mmol) was dissolved in 5.0 mL of Et_2O and taken into a Schlenk cuvette, which was connected to a Schlenk line and cooled to −80 °C; the initial UV–vis spectrum was recorded. With a long syringe needle, dioxygen was bubbled through the solution for 10 s, and excess dioxygen was removed carefully via evacuation and purging with argon. The 2,4,6-^{t}Bu$_3$-phenol solution was added, and the UV–vis spectrum recorded (yield ∼55%). The cold reaction solution was transferred to EPR sample tubes at −80 °C and immediately frozen at 77 K. The EPR spectra obtained confirmed formation of corresponding 2,4,6-^{t}Bu$_3$ phenoxyl radical and the presence of a copper(II) complex.

(31) Maiti, D.; Lucas, H. R.; Sarjeant, A. A. N.; Karlin, K. D. *J. Am. Chem. Soc.* **2007**, *129*, 6998–6999.

Reaction of $[\{(6tbp)Cu^{III}\}_2(O^{2-})_2](B(C_6F_5)_4)_2$ with Benzylamine. $[(6tbp)Cu^{I}]B(C_6F_5)_4$ (**7**) (0.045 g, 0.039 mmol) was dissolved in 5 mL of Et_2O solution inside the dry box, and this was taken into a 25 mL Schlenk flask. On the benchtop, this flask was cooled to −80 °C, and dioxygen bubbling led to $[\{(6tbp)Cu^{III}\}_2(O^{2-})_2](B(C_6F_5)_4)_2$, whereupon excess O_2 was removed. Benzylamine (0.004 g, 0.037 mmol) was added; the resulting mixture was bubbled with argon for 5 s, and the solution was kept at −80 °C for 3 h. The reaction solution was washed two times with pentane (20 mL), and the resulting supernatant was dried over Na_2SO_4. After the volume was reduced, GC and GC-MS analysis (Supporting Information Figure S10, see below, for conditions) confirmed the formation of benzonitrile (also, compared with authentic commercial benzonitrile) in ∼43% yield.

Reaction of $PhCH_2OH$ and $[(6tbp)Cu^{I}]^+/O_2$. In a 10 mL Schlenk flask, a 3 mL Et_2O solution of $[(6tbp)Cu^{I}]^+$ (**7**) (0.040 g, 0.034 mmol) was prepared in the glovebox. Following removal to the benchtop, O_2 bubbling (10 s) at −80 °C produced $[\{(6tbp)Cu^{III}\}_2(O^{2-})_2]^{2+}$ (**7-O_2**) (excess O_2 was removed). $PhCH_2OH$ (0.004 g, 0.037 mmol) was added to the copper solution, and the mixture was stirred for 2 h. A copper complex was precipitated by addition of pentane (20 mL). Washing was carried out as described above, and the collective pentane washes were dried over Na_2SO_4, filtered, concentrated, and subjected to GC and GC-MS analyses, which confirmed the formation of PhCHO in ∼80% yield.

Reaction of 9,10-Dihydroanthracene with $[\{(6tbp)Cu^{III}\}_2(O^{2-})_2]^{2+}$. $[\{(6tbp)Cu^{III}\}_2(O^{2-})_2](B(C_6F_5)_4)_2$ (excess O_2 removed) was prepared (at −80 °C) in a 25 mL Schlenk flask starting with $[(6tbp)Cu^{I}]^+$ (**7**) (0.043 g, 0.037 mmol) dissolved in 4 mL of Et_2O. 9,10-Dihydroanthracene (0.006 g, 0.033 mmol) was added, and the mixture was kept cold for 2 h. After the mixture was warmed to RT and left to sit for 6 h, rotary evaporation led to a concentrated solution of ∼0.3 mL. The copper complex was precipitated out by addition of 15 mL of pentane, and the mixture was washed two more times with 25 mL of pentane. The collective pentane washes were dried over Na_2SO_4, filtered, concentrated, and subjected to GC and GC-MS analyses (Supporting Information Figure S11 and Figure S12), which confirmed the formation of anthracene and anthraquinone in ∼10% and ∼15% yield, respectively.

Reaction of Xanthene with $[\{(6tbp)Cu^{III}\}_2(O^{2-})_2]^{2+}$. A solution of xanthene (0.005 g, 0.027 mmol) was prepared in 50 μL of Et_2O inside the glovebox. $[(6tbp)Cu^{I}]B(C_6F_5)_4$ (0.030 g, 0.025 mmol) was dissolved in 2.0 mL of Et_2O and taken in a 25 mL Schlenk flask. $[\{(6tbp)Cu^{III}\}_2(O^{2-})_2](B(C_6F_5)_4)_2$ (excess O_2 removed) was prepared at −80 °C, and the xanthene solution was added. After 5 h, the solution was warmed to RT. The resulting solution was concentrated to ∼0.2 mL, and the copper complex was precipitated by addition of 20 mL pentane. Additional pentane washes (2×, 15 mL each), drying over Na_2SO_4, filtration, concentration, and subjection to GC and GC-MS analyses (Figure S13), confirmed the formation of xanthone in ∼33% yield.

GC and GC-MS Analysis of the Reactions Above. All GC/MS experiments were carried out and recorded using a Shimadzu GC-17A/GCMS0QP5050 Gas Chromatograph/Mass Spectrometer. GC experiments were carried out and recorded using a Hewlett-Packard 5890 Series II Gas Chromatograph. The GC conditions for the product analysis were the following: injector port temp 250 °C; detector temp 250 °C; column temp, initial temp 80 °C, initial time 2 min, final temp 250 °C, final time, 25 min; gradient rate 30 °C/min; flow rate: 45 mL/min. The GC-MS conditions for the product analysis were the following: injector port temp 220 °C; detector temp 280 °C; column temp, initial temp 100 °C, initial time 2 min, final temp 250 °C, final time 25 min; gradient rate 10 °C/min; flow rate: 16 mL/min; ionization voltage: 1.5 kV.

Reaction of $[\{(6tbp)Cu^{III}\}_2(O^{2-})_2](B(C_6F_5)_4)_2$ (7-O_2) with TMPA. $[(6tbp)Cu^{I}]B(C_6F_5)_4$ (0.007 g, 0.006 mmol) was dissolved in 4.0 mL of Et_2O under argon in a UV–vis cuvette equipped with a glass stopper. This was cooled to −80 °C, and an initial spectrum was recorded. O_2 was bubbled to the copper(I) solution to form $[\{(6tbp)Cu^{III}\}_2(O^{2-})_2]^{2+}$ (**7-O_2**). Once the formation of **7-O_2** was complete, the cuvette assembly was attached to a vacuum line, and excess dioxygen was removed carefully via vacuum/argon cycles. While under a hard stream of Ar, the glass stopper was replaced with a rubber septum, and a TMPA (0.002 g, 0.007 mmol) solution was transferred anaerobically to the cuvette. An immediate solution color change occurred from yellowish brown to purple. To ensure mixing of the solution, a long syringe needle was inserted, and argon was purged through the solution (kept at −80 °C) for 5 s. Further addition of TMPA (0.002 g, 0.007 mmol) caused no change in spectrum recorded. Thus the addition of TMPA causes generation of species with absorption features at 525 nm, identical to that observed for solutions from $[(TMPA)Cu^{I}(CH_3CN)]^+/O_2$ reactivity. The percent conversion (∼90%) was calculated on the basis of the extinction coefficient of the peak at 525 nm and comparison to an authentic sample of $[(TMPA)Cu^{I}(CH_3CN)]^+/O_2$.

Addition of HCl to $[\{(6tbp)Cu^{III}\}_2(O^{2-})_2](B(C_6F_5)_4)_2$ (7-O_2). $[(6tbp)Cu^{I}]B(C_6F_5)_4$ (**7**) (0.020 g, 0.017 mmol) was dissolved in 5 mL of Et_2O under argon in a Schlenk flask equipped with a magnetic bar; the solution was cooled to −80 °C. O_2 was bubbled to the copper(I) solution to form $[\{(6tbp)Cu^{III}\}_2(O^{2-})_2]^{2+}$, and excess O_2 was removed carefully. HCl (34 μL) in Et_2O (Aldrich, 2 M) was added anaerobically to the flask using a plastic syringe; there was an immediate color change from yellowish brown to green. With a long needle, argon was purged through the solution for 5 s, and the solution was stirred for 30 min. Distilled water (15 mL) was added after the reaction solution was warmed to room temperature. The resulting mixture was stirred for 1 h at RT, and the aqueous layer was analyzed for H_2O_2 using $TiO(SO_4)$ test reagent[32–34] giving the result that hydrogen peroxide was formed in ∼80% yield. The

(32) Chufan, E. E.; Mondal, B.; Gandhi, T.; Kim, E.; Rubie, N. D.; Moenne-Loccoz, P.; Karlin, K. D. *Inorg. Chem.* **2007**, *46*, 6382–6394.

nonaqueous Et_2O layer (above) was washed three times with pentane (100 mL total), and the precipitate obtained was recrystallized from THF/pentane. The X-ray quality crystals obtained after vacuum drying (0.043 g, ~85%) were identified as $[\{(6tbp)Cu^{II}(Cl)\}_2](B(C_6F_5)_4)_2$ (Figure S4, Supporting Information).

Resonance Raman (rR) Spectroscopy. Resonance Raman spectroscopic measurements were undertaken using a Princeton Instruments ST-135 back-illuminated CCD detector on a Spex 1877 CP triple monochromator with 1200, 1800, and 2400 grooves/mm holographic spectrograph gratings. The excitation was provided by Coherent 190C−K Kr+ and Innova Sabre 25/7 Ar+ CW lasers. The spectral resolution was <2 cm^{-1}. Sample concentrations were approximately 0.4 mM in copper−dioxygen complexes and were run at 77 K in a liquid N_2 finger Dewar (Wilmad). Samples were prepared in dried solvents in standard low-grade NMR tubes. In Baltimore, the precursor copper(I) sample solutions prepared in the glovebox in NMR tubes under N_2 were cooled to −80 °C on the benchtop and then subjected to O_2 bubbling via syringe. Samples employing $^{18}O_2$ in 25 mL break-seal flasks (ICON Services, NJ) were prepared as previously described in detail.[35]

Results and Discussion

Ligand Synthesis. The syntheses of L^{CH_2OMe},[27] $L^{N(CH_3)_2}$,[28] and 6tBP[31] (Chart 2) were previously reported. $L^{NH(CH_3)}$ (Chart 2) was obtained from oxidative N-dealkylation chemistry of copper(II)−hydroperoxo species of $L^{N(CH_3)_2}$.[28] Generation of $L^{N(CH_3)_2}$ and $L^{N(CH_2Ph)_2}$ (Chart 2) involves pressure tube reaction of BrTMPA with dimethylamine or dibenzylamine, respectively, under basic conditions (see Supporting Information). The ligands 6PhTPA ((6-phenyl-2-pyridylmethyl)bis(2-pyridylmethyl)amine), by Canary and co-workers[12] and Que and co-workers,[36] 6MeTMPA by Suzuki and co-workers,[37,38] MAPA ((6-amino-2-pyridylmethyl)bis(2-pyridylmethyl)amine),[39] MPPA ((6-^{t}Butylacetamido-2-pyridyl-methyl)bis(2-pyridylmethyl)amine) by Masuda and co-workers,[40] and BPQA ((2-quinolylmethyl)bis(2-pyridylmethyl)amine) by Karlin and co-workers[41–43] were previously reported.

Copper(I) and Copper(II) Complexes. Mononuclear copper(I) complexes not previously reported are $[(L^{NH(CH_3)})Cu^I]^+$ (**2**) and $[(L^{N(CH_2Ph)_2})Cu^I]^+$ (**10**) (Chart 2) which were synthesized under an argon atmosphere by combination of equimolar mixtures of the respective tetradentate ligand and $[Cu^I(CH_3CN)_4]B(C_6F_5)_4$[29] in THF. Isolation of solids was achieved by addition of pentane, and this was followed by recrystallization (see Experimental Section). In connection with ligands generated in our own laboratories and related to the present study involving dioxygen reactivity, copper(I) compounds $[(L^{CH_2OMe})Cu^I]^+$ (**1**) (X-ray),[27] $[(BPQA)Cu^I]^+$ (**6**),[41–43] $[(6tbp)Cu^I]^+$ (**7**) (X-ray),[31] and $[(L^{N(CH_3)_2})Cu^I]^+$ (**9**)[28] have previously been reported.

It has always been very useful to generate and characterize copper(II) complex analogues of the copper(I) ligand compounds, for example, to deduce copper(II) coordination geometries that may relate to copper−dioxygen complexes.[30,44] The following have previously been reported and characterized by X-ray crystallography: $[\{(L^{CH_2OMe})Cu^{II}(Cl)\}_2]^{2+}$,[27] $[\{(L^{CH_2OMe})Cu^{II}(Br)\}_2]^{2+}$,[27] $[(L^{NH(CH_3)})Cu^{II}(Cl)]^+$,[28] $[(BPQA)Cu^{II}(Cl)]^+$,[41,42] $[(6tbp)Cu^{II}(acetone)]^{2+}$,[31] and $[(L^{N(CH_3)_2})Cu^{II}(H_2O)]^{2+}$.[28] In the Supporting Information, we also report the X-ray structures of $[\{(6tbp)Cu^{II}(Cl)\}_2](B(C_6F_5)_4)_2$ and $[\{(L^{N(CH_2Ph)_2})Cu^{II}(Cl)\}_2](B(C_6F_5)_4)_2$, generated by copper(I) ligand complex exposure to chloroform,[30] a very useful procedure with which to readily obtain chloride copper(II) complexes which typically crystallize.[41,42]

$[(L)Cu^{II}_2(\mu\text{-}1,2\text{-}O_2^{2-})]^{2+}$ (A) Complex Formation with Group I Ligand−Copper Complexes. As stated in the Introduction, these ligand−copper complexes (Chart 2) form (μ-1,2)-peroxodicopper(II) products (**A**, Charts 1 and 2), following oxygenation of ligand−copper(I) precursors in THF solvent at −80 °C. For $[(L^{CH_2OMe})Cu^I]B(C_6F_5)_4$ (**1**), we previously reported that the colorless copper(I) solution changes to the purple species that was formulated as $[\{(L^{CH_2OMe})Cu^{II}\}_2(\mu\text{-}1,2\text{-}O_2^{2-})]^{2+}$ (**1-O$_2$**), {$\lambda_{max} = 540$ nm (ϵ, 9550 $M^{-1}cm^{-1}$) and 610 nm, sh, (ϵ, 6500 $M^{-1}cm^{-1}$)} (Figure 1a).[27] These features closely resemble the distinctive pattern known for the parent complex $[\{(TMPA)Cu^{II}\}_2(\mu\text{-}1,2\text{-}O_2^{2-})]^{2+}$ (**A1**) and other O_2-adducts with similar structures.[6] Confirmation, reported here for the first time, comes from resonance Raman (rR) spectroscopic data (Figure 1b), where the O−O (848 cm^{-1}), symmetric Cu−O (550 cm^{-1}), and antisymmetric Cu−O (508 cm^{-1}) stretching vibrations are readily observable and confirmed by experiments carried out using $^{18}O_2$ to form the complexes. These data and corresponding information for other complexes are given in Table 1.

The absorption spectrum of $[\{(L^{CH_2OMe})Cu^{II}\}_2(\mu\text{-}1,2\text{-}O_2^{2-})]^{2+}$ (**1-O$_2$**) shows a decreased peroxide $\pi_\sigma^* \rightarrow d_\sigma$ charge-transfer band energy as compared to that of $[\{(TMPA)Cu^{II}\}_2(\mu\text{-}1,2\text{-}O_2^{2-})]^{2+}$ (**A1**) (**1-O$_2$**, 540 nm; **A1**, 523 nm),[8]

(33) Chaudhuri, P.; Hess, M.; Mueller, J.; Hildenbrand, K.; Bill, E.; Weyhermueller, T.; Wieghardt, K. *J. Am. Chem. Soc.* **1999**, *121*, 9599–9610.
(34) Eisenberg, G. M. *Ind. Eng. Chem., Anal. Ed.* **1943**, *15*, 327–328.
(35) Maiti, D.; Fry, H. C.; Woertink, J. S.; Vance, M. A.; Solomon, E. I.; Karlin, K. D. *J. Am. Chem. Soc.* **2007**, *129*, 264–265.
(36) Jensen, M. P.; Que, E. L.; Shan, X. P.; Rybak-Akimova, E.; Que, L. *Dalton Trans.* **2006**, 3523–3527.
(37) Nagao, H.; Komeda, N.; Mukaida, M.; Suzuki, M.; Tanaka, K. *Inorg. Chem.* **1996**, *35*, 6809–6815.
(38) Uozumi, K.; Hayashi, Y.; Suzuki, M.; Uehara, A. *Chem. Lett.* **1993**, 963–966.
(39) Wada, A.; Honda, Y.; Yamaguchi, S.; Nagatomo, S.; Kitagawa, T.; Jitsukawa, K.; Masuda, H. *Inorg. Chem.* **2004**, *43*, 5725–5735.
(40) Yamaguchi, S.; Wada, A.; Funahashi, Y.; Nagatomo, S.; Kitagawa, T.; Jitsukawa, K.; Masuda, H. *Eur. J. Inorg. Chem.* **2003**, 4378–4386.
(41) Wei, N.; Murthy, N. N.; Chen, Q.; Zubieta, J.; Karlin, K. D *Inorg. Chem.* **1994**, *33*, 1953–1965.
(42) Wei, N.; Murthy, N. N.; Karlin, K. D. *Inorg. Chem.* **1994**, *33*, 6093–6100.
(43) Lee, D.-H.; Wei, N.; Murthy, N. N.; Tyeklár, Z.; Karlin, K. D.; Kaderli, S.; Jung, B.; Zuberbühler, A. D. *J. Am. Chem. Soc.* **1995**, *117*, 12498–12513.
(44) Schatz, M.; Becker, M.; Thaler, F.; Hampel, F.; Schindler, S.; Jacobson, R. R.; Tyeklár, Z.; Murthy, N. N.; Ghosh, P.; Chen, Q.; Zubieta, J.; Karlin, K. D. *Inorg. Chem.* **2001**, *40*, 2312–2322.
(45) Yamaguchi, S.; Nagatomo, S.; Kitagawa, T.; Funahashi, Y.; Ozawa, T.; Jitsukawa, K.; Masuda, H. *Inorg. Chem.* **2003**, *42*, 6968–6970.

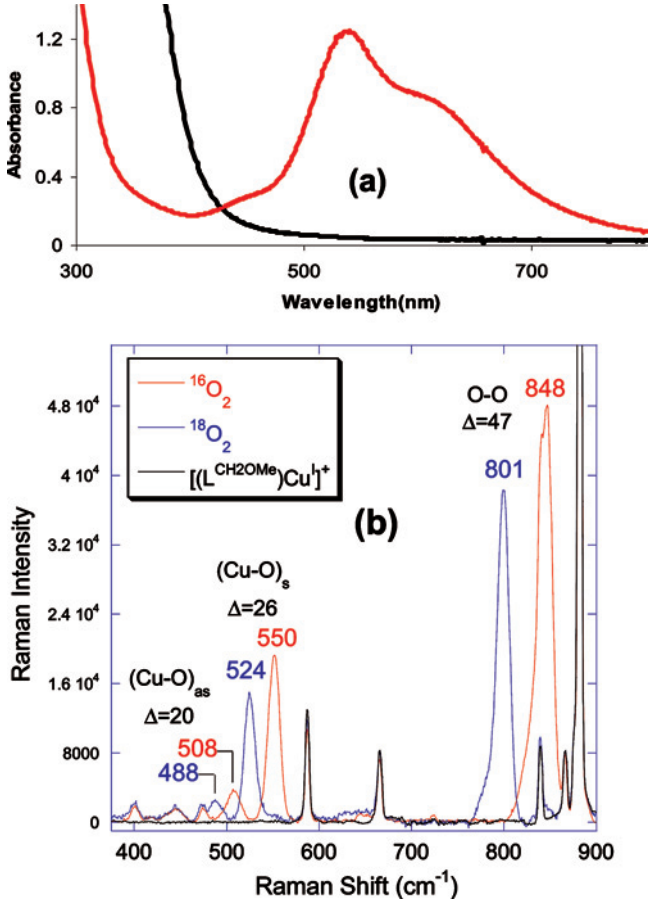

Figure 1. (a) UV–vis spectra at −80 °C in THF, illustrating formation of the **1-O$_2$** (**red** spectrum) formed from [(L^{CH_2OMe})Cu^{I}]$^+$ (**1**) (**black** spectrum) following bubbling with O$_2$. (b) rR spectrum of [(L^{CH_2OMe})Cu^{I}]$^+$ (**1**) (black), **1-^{16}O$_2$-**(B(C$_6$F$_5$)$_4$)$_2$ (**red**), and **1-^{18}O$_2$-**(B(C$_6$F$_5$)$_4$)$_2$ (**blue**) (λ_{excit} = 620 nm at 77 K).

and the rR spectrum shows a lower (Cu−O)$_s$ stretch (**1-O$_2$**, 550 cm^{-1}; **A1**, 561 cm^{-1}.[8,23,27] These data indicate the Cu−O bonds of **1-O$_2$** are weaker than those of [{(TMPA)Cu^{II}}$_2$(μ-1,2-O$_2^{2-}$)]$^{2+}$ (**A1**). A possible explanation for this Cu−O bond weakening is a square pyramidal distortion of the Cu(II) ligand field. The steric congestion in L^{CH_2OMe} arising from the presence of a 6-substituent at one of the pyridyl arms of the TMPA parent chelate results in a square pyramidal distortion of the ligand in [{(L^{CH_2OMe})Cu^{II}(Br)}$_2$](B(C$_6$F$_5$)$_4$)$_2$.[27] In a square pyramidal complex, three of the chelate ligands would donate into Cu's $d_{x^2-y^2}$ orbital thus reducing the donation from the peroxo to the Cu and the strength of this bond. The (Cu−O)$_{as}$ stretch is also observed for this **1-O$_2$** system (at 508 cm^{-1}) which further supports distortion of the complex such that it no longer has a center of inversion.

While the $\pi_\sigma^* \rightarrow d_\sigma$ charge transfer and (Cu−O)$_s$ stretch are shifted down in energy; the O−O stretch has increased in energy (**1-O$_2$**, 848 cm^{-1}; **A1**, 832 cm^{-1}).[8] The decreased peroxo π_σ^* donation to Cu would result in more electron density in the peroxo antibonding π_σ^* orbital, thus a weaker, not stronger, O−O bond. The square pyramidal structural distortion considered above would increase steric interactions between ligands to the two Cu's, potentially resulting in an increased Cu−Cu distance. This could increase the Cu−O−O angle relative to that in [{(TMPA)Cu^{II}}$_2$(μ-1,2-O$_2^{2-}$)]$^{2+}$. As this angle increases to greater than 120°, mechanical mixing of the Cu−O and O−O modes would occur which could result in a higher O−O stretching frequency even with a small decrease in O−O bond strength.[46]

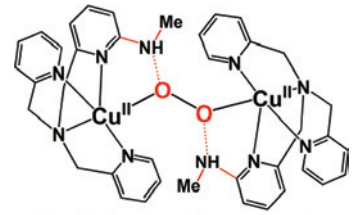

H-bonding in *trans*-μ-1,2-peroxo complex
[{(L$^{NH(CH3)}$)Cu^{II}}$_2$(μ-1,2-O$_2^{2-}$)]$^+$ (**2-O$_2$**)

A THF solution of [(L$^{NH(CH_3)}$)Cu^{I}]B(C$_6$F$_5$)$_4$ (**2**) at −80 °C reacts with O$_2$ leading to a reddish-brown solution with prominent UV–vis features at λ_{max} = 498 nm (ϵ, 7500 M^{-1} cm^{-1}) and 635 nm (ϵ, 1700 M^{-1} cm^{-1}). Again, the UV–vis charge-transfer pattern and rR data (vide infra) (Figure 2a and b) support the formulation as [{(L$^{NH(CH_3)}$)Cu^{II}}$_2$(μ-1,2-O$_2^{2-}$)]$^{2+}$ (**2-O$_2$**). There is a considerable increase in the peroxo $\pi_\sigma^* \rightarrow$ Cu d_σ charge-transfer energy as compared to the parent compound [{(TMPA)Cu^{II}}$_2$(μ-1,2-O$_2^{2-}$)]$^{2+}$ (**A1**) (Table 1). Masuda and co-workers[39,40] have accounted for such effects within a series of closely related ligand−copper−dioxygen complexes possessing intramolecular H-bonding interactions. For **2-O$_2$**, H-bonding from the N(H)CH$_3$ group of L$^{NH(CH_3)}$ to the peroxo moiety (see diagram below) would effect these changes. This H-bonding would result in stabilization of the peroxo π_σ^* orbital leading to a larger d_σ (Cu) and π_σ^* (O$_2^{2-}$) energy separation and thus an increase in the $\pi_\sigma^* \rightarrow d_\sigma$ charge-transfer energy.

The O−O and Cu−O stretching vibrations for **2-O$_2$** occur at 849 ($\Delta(^{18}O_2)$ = –47) and 544 ($\Delta(^{18}O_2)$ = –25) cm^{-1}, respectively (Table 1). The rR spectral behavior of **2-O$_2$** can also be interpreted in terms of the contribution of the hydrogen bonding of the NH group introduced into the pyridine 6-position of parent TMPA (diagram above). The H-bonding interaction would decrease the lone-pair repulsion in the peroxide, strengthening the O−O bond (higher O−O stretch)[47] while weakening the Cu−O bond, in comparison to systems that do not have such H-bonding (Table 1).

We note that unlike the behavior found for other O$_2$-adducts with tetradentate N$_4$ ligands possessing structure **A**,[6,9,43,48,49] the O$_2$-binding and formation of **2-O$_2$** appears to be irreversible. Warming, CO bubbling, or both did not lead to release of O$_2$ and regeneration of [(L$^{NH(CH_3)}$)Cu^{I}]$^+$ (**2**).

(46) Brunold, T. C.; Tamura, N.; Kitajima, N.; Moro-Oka, Y.; Solomon, E. I. *J. Am. Chem. Soc.* **1998**, *120*, 5674–5690.
(47) Root, D. E.; Mahroof-Tahir, M.; Karlin, K. D.; Solomon, E. I. *Inorg. Chem.* **1998**, *37*, 4838–4848.
(48) Karlin, K. D.; Wei, N.; Jung, B.; Kaderli, S.; Zuberbühler, A. D. *J. Am. Chem. Soc.* **1991**, *113*, 5868–5870.
(49) Tyeklár, Z.; Jacobson, R. R.; Wei, N.; Murthy, N. N.; Zubieta, J.; Karlin, K. D. *J. Am. Chem. Soc.* **1993**, *115*, 2677–2689.

Table 1. Summary of Spectroscopic Features for Binuclear Copper−Dioxygen Adducts

μ-1,2-peroxodicopper(II) complexes with type I ligands	solvent	UV–vis/nm (ϵ/M^{-1} cm^{-1})	ν/cm^{-1}, ^{16}O−^{16}O (^{18}O−^{18}O)	ν/cm^{-1}, Cu−^{16}O (Cu−^{18}O)	ref
[{(TMPA)Cu^{II}}$_2$(μ-1,2-O$_2^{2-}$)]$^{2+}$ (**A1**)	EtCN	525 (11 300), 615(58 00)	832 (788)	561 (535)	18
(parent complex)	Et$_2$O	520 (19 200)	827 (783)	561 (535)	23
[{(L^{CH_2OMe})Cu^{II}}$_2$(μ-1,2-O$_2^{2-}$)]$^{2+}$ (**1-O$_2$**)	THF	540 (9550), 610 (6500)	848 (801)	550 (524)	*a*
[{(L$^{NH(CH_3)}$)Cu^{II}}$_2$(μ-1,2-O$_2^{2-}$)]$^{2+}$ (**2-O$_2$**)^d	THF	498 (7500), 635 (1700)	849 (802)	544 (519)	*a*
[{(6MeTMPA)Cu^{II}}$_2$(μ-1,2-O$_2^{2-}$)]$^{2+}$ (**3-O$_2$**)	acetone	537 (5500), 600 (4000)	*b*	*b*	27
[{(MAPA)Cu^{II}}$_2$(μ-1,2-O$_2^{2-}$)]$^{2+}$ (**4-O$_2$**)^d	acetone	503 (7500), 600 (1500)	847 (800)	544 (518)	39
[{(MPPA)Cu^{II}}$_2$(μ-1,2-O$_2^{2-}$)]$^{2+}$ (**5-O$_2$**)^d	acetone	517 (5600), 600 (1500)	837 (792)	*b*	40
[{(BPQA)Cu^{II}}$_2$(μ-1,2-O$_2^{2-}$)]$^{2+}$(**6-O$_2$**)	EtCN	535 (8600), 600	*b*	*b*	41

bis(μ-oxo)dicopper(III) complexes with type II ligands	solvent	UV–vis/nm (ϵ/M^{-1} cm^{-1})	ν/cm^{-1} (Cu−^{16}O)	ν/cm^{-1} (Cu−^{18}O)	ref
[{(6tbp)Cu^{III}}$_2$(O^{2-})$_2$]$^{2+}$ (**7-O$_2$**)	CH$_2$Cl$_2$	383 (Et$_2$O, ≥7000)^e	594	568	*a*
[{(6PhTPA)Cu^{III}}$_2$(O^{2-})$_2$]$^{2+}$ (**8-O$_2$**)	acetone	378	599	573	36
[{(L$^{N(CH_3)_2}$)Cu^{III}}$_2$(O^{2-})$_2$]$^{2+}$ (**9-O$_2$**)	Et$_2$O	383 (18 900)^c	*c*	*c*	*a*, 28
[{(L$^{N(CH_2Ph)_2}$)Cu^{III}}$_2$(O^{2-})$_2$]$^{2+}$ (**10-O$_2$**)	acetone	390 (5300)	598	572	*a*

^{a} This work. ^{b} Not reported. ^{c} Not detected. ^{d} these possess intramolecular H-bonding to the peroxo group, see text. ^{e} See text.

Bis(μ-oxo)dicopper(III) Complex [(L)Cu$^{III}_2$(O^{2-})$_2$]$^{2+}$ (C) Formation with Group II Ligand−Copper Complexes. Reaction of O$_2$ with Copper(I) Complexes of 6tBP, L$^{N(CH_3)_2}$, and L$^{N(CH_2Ph)_2}$. As previously described in a qualitative manner, bubbling O$_2$ through −80 °C Et$_2$O or THF solutions of [(6tbp)Cu^{I}]B(C$_6$F$_5$)$_4$ (**7**) or [(L$^{N(CH_3)_2}$)Cu^{I}]B(C$_6$F$_5$)$_4$ (**9**) (Chart 1) results in immediate color changes from light to bright brownish-yellow and EPR silent solutions of [{(6tbp)Cu^{III}}$_2$(O^{2-})$_2$]$^{2+}$ (**7-O$_2$**) {λ_{max} (Et$_2$O) = 383 nm ($\epsilon \geq 7000$ M^{-1} cm^{-1}), Figure 3a}[31] or [{(L$^{N(CH_3)_2}$)Cu^{III}}$_2$(O^{2-})$_2$]$^{2+}$ (**9-O$_2$**) {λ_{max} = 383 nm (ϵ = 18900 M^{-1} cm^{-1}) (Table 1).[28,50] The structure assignment as **C** (Scheme 1, Chart 2) for **7-O$_2$** and **9-O$_2$** (vide infra) comes from the characteristic[5,6] UV–vis spectra of this structure, along with rR data given below. Formation of **7-O$_2$** can be performed in a wide range of solvents, for example,

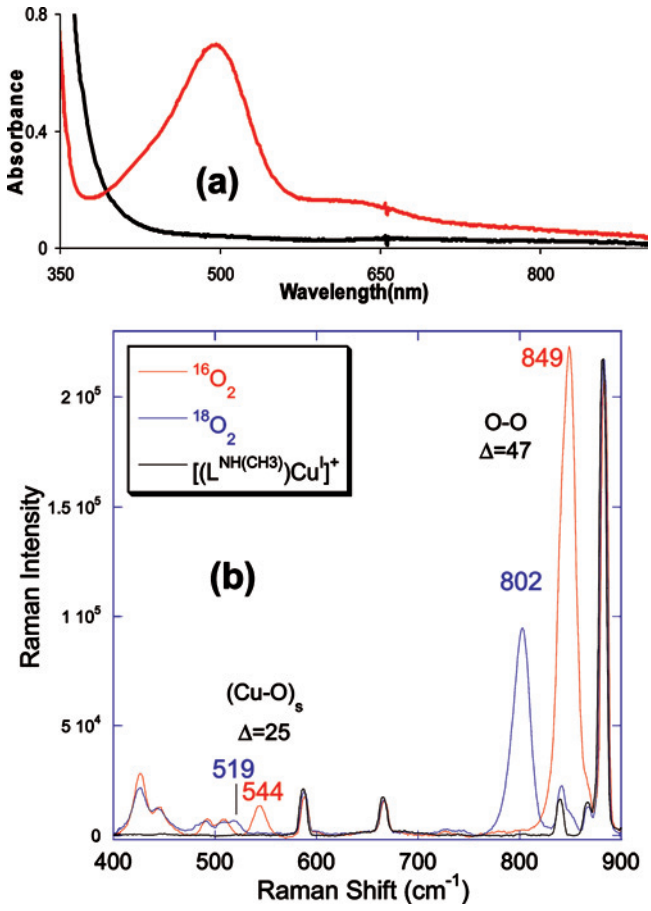

Figure 2. (a) UV–vis spectra at −80 °C in THF, illustrating formation of μ-1,2-peroxodicopper(II) complex (**2-O$_2$**) (**red** spectrum), formed from the [(L$^{NH(CH_3)}$)Cu^{I}]$^{+}$ (**2**) (**black** spectrum) reaction with O$_2$, and possessing H-bonding (see text). (b) rR spectrum of [(L$^{NH(CH_3)}$)Cu^{I}]$^{+}$ (**black**), **2**-^{16}O$_2$-(B(C$_6$F$_5$)$_4$)$_2$ (**red**), and **2**-^{18}**O$_2$**-(B(C$_6$F$_5$)$_4$)$_2$ (**blue**) (λ_{excit} = 501.7 nm at 77 K).

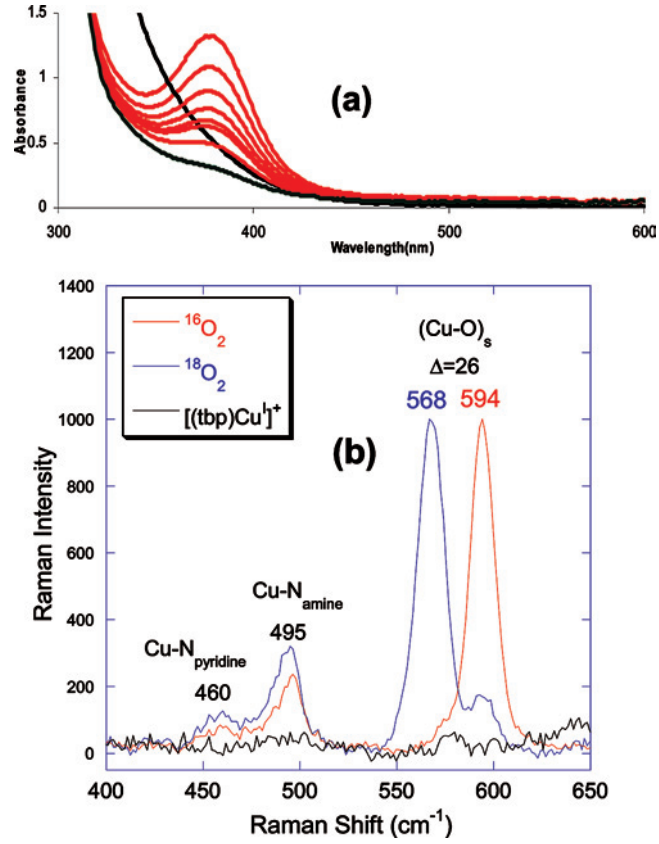

Figure 3. (a) UV–vis spectra at −80 °C in Et$_2$O, illustrating formation of **7-O$_2$** (**red** spectrum) from O$_2$ reaction with [(6tbp)Cu^{I}]$^{+}$ (**7**) (**black** spectrum). A **7-O$_2$** decomposition product (**green** spectrum at −80 °C) forms in ~20 min. (b) rR spectrum (ν_{Cu-O} region) of **7-O$_2$**-(B(C$_6$F$_5$)$_4$)$_2$ with ^{16}O$_2$ (**red**) or ^{18}O$_2$ (**blue**) {CH$_2$Cl$_2$ solvent, λ_{excit} = 386 nm, 77 K}.

(50) See Supporting Information.

acetone, CH_2Cl_2, Et_2O, THF, propionitrile, toluene, and ethylbenzene. However it is relatively unstable and decomposes within ~ 20 min (Figure 3a) in all these solvents except Et_2O. Studies in the latter solvent allowed us to at least provide a lower limit for the extinction coefficient (given above).

For **7-O_2**, a strong peak at 594 cm^{-1} which shifts to 568 cm^{-1} upon isotopic substitution with $^{18}O_2$ is observed in rR spectra (Figure 3b). This can be assigned as a ν(Cu−O) stretching vibration, consistent with the formulation of the copper complex as having a bis(μ-oxo)dicopper(III) structure (**C**).[6] The data further show that there is a less strongly enhanced band at 1188 cm^{-1} that is twice the frequency compared to the strong ν(Cu−O) stretch (594 cm^{-1}); with O-18-labeling, this shifts to 1135 cm^{-1}, which is nearly twice that of the value for the ν(Cu−^{18}O) stretch (Figure S14 in Supporting Information). Thus, this band is assigned as the overtone of the ν(Cu−O) mode. In addition, ν(Cu−N) modes are observed (Figure 3b) from the equatorially bound pyridine ($\nu(Cu-N_{pyridine}) = 460\ cm^{-1}$) and equatorially bound amine ($\nu(Cu-N_{amine}) = 495\ cm^{-1}$) of **7-$O_2$**.[23]

Que and co-workers[36] previously described UV–vis and rR characterization (Table 1) of the bis(μ-oxo)dicopper(III) species, $[\{(6\text{-PhTPA})Cu^{III}\}_2(O^{2-})_2]^{2+}$ (**8-O_2**) (Chart 2), which is very closely related to our own system with 6tBP (but without the tBu group), described above.

For $[\{(L^{N(CH_3)_2})Cu^{III}\}_2(O^{2-})_2]^{2+}$ (**9-O_2**), the characteristic UV–vis spectrum obtained readily leads to its formulation.[6,28] The complex was found to be unstable for rR interrogation at 77 K, perhaps because of photochemical decomposition; therefore, we were unable to obtain rR data for further confirmation. For this and other reasons,[51] we synthesized a close analogue $L^{N(CH_2Ph)_2}$ and a copper(I) complex of this ligand (Chart 2). The O_2-reactivity of $[(L^{N(CH_2Ph)_2})Cu^{I}]B(C_6F_5)_4$ (**10**) is very similar to that for the dimethyl analogue **9**. Here, low-temperature UV–vis[50] and rR data (Figure 4) could be obtained (Table 1), thus proving the bis(μ-oxo)dicopper(III) complex formulation, $[\{(L^{N(CH_2Ph)_2})Cu^{III}\}_2(O^{2-})_2]^{2+}$ (**10-O_2**).

Summary: Group I versus Group II (Chart 2) Tetradentate Ligand-Copper Complexes and their O_2 Adduct Structural Preferences. In this report, we have elucidated the O_2-adduct structures obtained with copper(I) complexes with two ligands of Group I. From previous literature, four further examples of TMPA-like ligands with one pyridyl (or quinolyl) group possessing a 6-substituent of the -XHR type (see Chart 2) are copper(I) complexes which react with O_2 to form (μ-1,2)peroxodicopper(II) structures (**A**). Three new examples of Group II ligand-copper complex O_2-chemistry have been described here, all forming a (bis-μ-oxo)dicopper(III) complex when the single pyridyl group has a -XR_2 substituent (Chart 2) {also see Table 1}. Data for the closely related complex **8-O_2** (Chart 2) are also provided in Table 1.

As stated in the Introduction, tetradentate ligands with nitrogen donors tend to form (μ-1,2)peroxodicopper(II) structures (**A**), most likely because copper(II) complexes with overall pentacoordinate structures are stable and common.[52,53] For symmetrically disposed, tripodal tetradentate ligands, trigonal bipyramidal pentacoordiante copper(II) complexes generally form.[42,54] However, when steric interactions become important, the presence of a 6-position substituent (adjacent to the N-atom) of a pyridyl ring, for example, the structure can distort. As detailed here, it takes a 6-XR_2 substituent and not just a 6-XHR substituent to effect such a change. In the O_2 adducts of the type discussed in this report, the O−O bond breaks as elongated Cu−N bond distances result from the presence of a 6-pyridyl substituent,[30] leading to a stable essentially square-planar $Cu^{III}_2(O^{2-})_2$ structure. As mentioned (Introduction), this has been proven directly for the case of the copper−dioxygen adduct with the ligand Me_2TPA (Chart 1).[10] Also, our interpretations are consistent with ligand effect results observed and summarized by Itoh and co-workers,[1,55] that is, that bis(2-pyridylmethyl)amine tridentate ligands afford (bis-μ-oxo)dicopper(III) complexes when copper(I) precursors are oxygenated at a low temperature.

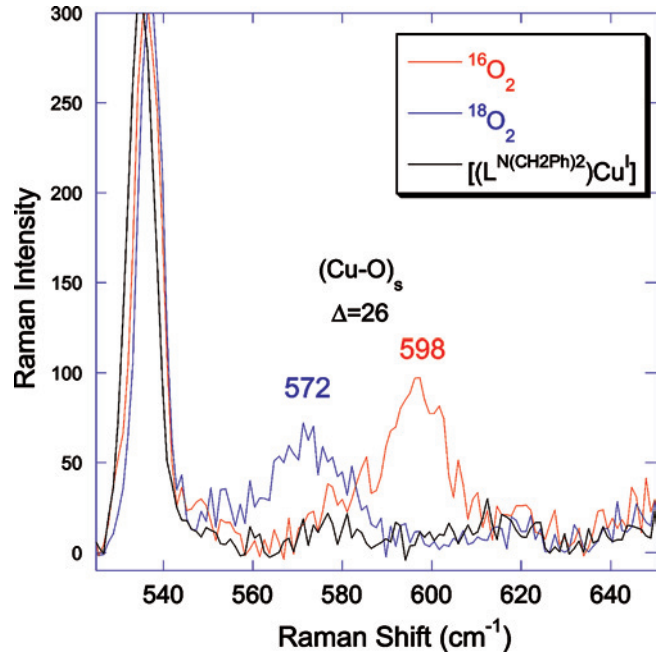

Figure 4. rR spectrum of $[(L^{N(CH_2Ph)_2})Cu^{I}]B(C_6F_5)_4$ (black) and **10-O_2**-$(B(C_6F_5)_4)_2$ formed using $^{16}O_2$ (**red**) or $^{18}O_2$ (**blue**) {acetone solvent, λ_{excit} = 380 nm, 77 K}.

Exogenous Substrate Reactivity with the Bis(μ-oxo)-dicopper(III) Complex $[\{(6tbp)Cu^{III}\}_2(O^{2-})_2]^{2+}$ (7-O_2). We recently reported quite interesting new chemistry when generating hydroperoxo complexes starting with copper(II) derivatives of either 6tBP or $L^{N(CH_3)_2}$ (Chart 2).[28,31] The aryl hydroxylation chemistry for the former, or the

(51) The oxidative N-dealkylation chemistry of copper complexes with this ligand will be reported elsewhere.

(52) Hathaway, B. J. Copper. In *Comprehensive Coordination Chemistry*; Wilkinson, G., Ed.; Pergamon: New York, 1987; Vol. *5*; pp 533–774.
(53) Kim, E.; Chufán, E. E.; Kamaraj, K.; Karlin, K. D. *Chem. Rev.* **2004**, *104*, 1077–1133.
(54) Karlin, K. D.; Hayes, J. C.; Shi, J.; Hutchinson, J. P.; Zubieta, J. *Inorg. Chem.* **1982**, *21*, 4106–4108.
(55) Osako, T.; Ueno, Y.; Tachi, Y.; Itoh, S. *Inorg. Chem.* **2003**, *42*, 8087–8097.

Scheme 2

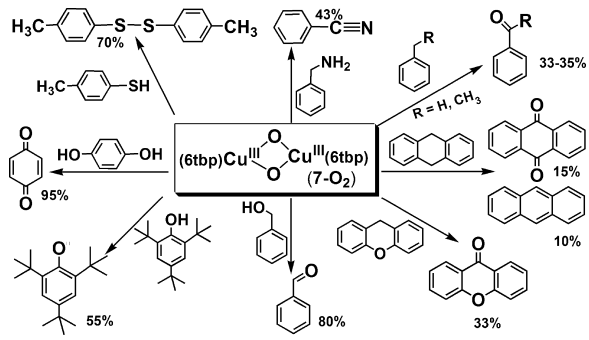

oxidative N-dealkylation chemistry in the latter system are not effected by the related copper(I)−dioxygen adducts described here, that is, bis-μ-oxodicopper(III) complexes $[\{(6tbp)Cu^{III}\}_2(O^{2-})_2]^{2+}$ (**7-O$_2$**) or $[\{(L^{N(CH_3)_2})Cu^{III}\}_2(O^{2-})_2]^{2+}$ (**9-O$_2$**).[28,31] While reactivity studies with bis(μ-oxo)dicopper(III) entities are reasonably well-known,[5,7,56] we wished to round out studies of these singly pyridyl 6-substituted complexes. Here, we report such investigations with **7-O$_2$**, as one example that we chose to study in some detail (vide infra). For ligand complexes from our own laboratories (**1**, **2**, **6**, **9**, and **10**, Chart 2), reactivity studies with exogenous substrates have not been examined, while as far as we are aware (via searching the literature), the same is true for $2Cu^I/O_2$ derived complexes for **3–5** and **8**.

Reaction of 7-O$_2$ with ArSH, PhCH$_2$OH, and ArCH$_2$NH$_2$ Substrates. After removal of excess dioxygen from solutions of bis(μ-oxo)dicopper(III) complex **7-O$_2$** at −80 °C, 1–3 equiv of various substrates were added. After workup, the organic products were characterized by GC and GC-MS spectrometry (see Experimental Section), and the results are summarized in Scheme 2. Reactions of thiocresol, benzyl alcohol, benzylamine, and tetrahydrofuran produce 4-methylphenyl disulfide, benzaldehyde, benzonitrile, and 2-hydroxytetrahydrofuran (along with γ-butyrolactone), respectively. $[\{(6tbp)Cu^{III}\}_2(O^{2-})_2]^{2+}$ (**7-O$_2$**) reacts with xanthene to give xanthone, and 9,10-dihydroanthracene leads to the production of anthracene and anthraquinone. Unreacted starting material substrates constitute the only other materials isolated or detected in these reactions (Scheme 2). The reactions with phenols, toluene, and ethylbenzene are described below.

Reaction of 7-O$_2$ with Phenolic Substrates. Upon addition of an anaerobic solution of 2,4,6-^{t}Bu$_3$-phenol to a −80 °C solution of $[\{(6tbp)Cu^{III}\}_2(O^{2-})_2]^{2+}$ (**7-O$_2$**) (excess O_2 removed), there is an immediate change in its UV–vis spectrum (Figure 5, yield ∼55%). The strong band at 383 nm from **7-O$_2$** disappears, and a new broad peak appears at ∼360 nm ($\epsilon \approx 2150$ M^{-1} cm^{-1}) accompanied by sharp feature at 405 nm (Figure 5, inset); the latter is characteristic[57] of the 2,4,6-^{t}Bu$_3$ phenoxyl radical. Aliquots of this −80 °C solution were transferred to EPR sample tubes and immediately frozen at 77 K. EPR spectra exhibited the typical $g \approx 2$ radical signal, accompanied by absorptions typical for copper(II) ion complexes (Figure 6). We suggest that this latter only moderately stable (at −80 °C; UV–vis criterion, Figure 5) species arises as a direct result of phenol H-atom abstraction by **7-O$_2$**, possibly giving the binuclear complex $[\{(6tbp)_2Cu^{II}Cu^{III}\}(O^{2-})(OH^-)]^{2+}$ (**7-O$_2$−H**) (Scheme 3). However, the four-line EPR spectrum and lack of a half-field ($M_s = 2$ transition at $g \approx 4$) transition suggests that a mononuclear rather than binuclear species is present. In case the spectrum represented a localized mixed-valent form of **7-O$_2$−H**, we hoped we might observe a delocalized structure and seven-line spectrum by recording EPR spectra at higher temperatures; however, the thermal instability of this EPR active copper entity thwarted our efforts. Such an initial mixed-valent dicopper product formed following $Cu^{III}_2(O^{2-})_2$ abstraction of a substrate H-atom has been previously hypothesized[7,20,25,56,58–61] and suggested by computational studies[58,62,63] to have a reasonable stability; however, no experimental evidence, spectroscopic or structural, has yet been provided. It is interesting to note that Itoh and co-workers[60] have also speculated that such a binuclear complex product, $[\{(ligand)_2Cu^{II}Cu^{III}\}(O^{2-})(OH^-)]^{2+}$, might split into mononuclear species including $[(ligand)Cu^{II}-OH]^{1+}$, which would likely give rise to an EPR signal like that which we observe. More studies are needed.

The bis(μ-oxo)dicopper(III) complex **7-O$_2$** was also reacted with 2,4-^{t}Bu$_2$-phenol and 1,4-hydroquinone. With the former substrate, the typically observed 2,4-^{t}Bu$_2$-phenol oxidatively coupled dimer forms (50% yield).[31] With hydroquinone, 1,4-benzoquinone could be isolated in high yield (∼95%) (Scheme 2).

Thus, as seen for many other $Cu^{III}_2(O^{2-})_2$ complexes,[5,7] **7-O$_2$** appears to effect hydrogen-atom abstraction reactions and acts as an overall two-electron oxidant. This conclusion is further supported by the more detailed study carried out involving toluene as substrate.

Toluene and Ethylbenzene Oxygenation with $[\{(6tbp)Cu^{III}\}_2(O^{2-})_2]^{2+}$ (7-O$_2$). To our knowledge, neither toluene nor ethylbenzene have previously been examined as substrates for copper(I)/O_2 derived oxidants. We find that **7-O$_2$** oxidizes toluene or ethylbenzene (as solvents) to benzaldehyde (∼33%) and acetophenone (∼35%), respectively. The yields given are on a per dicopper basis. As will be described here, the nature of these reactions are consistent with that of monooxygenase-type chemistry where the result of a 2 Cu(I)/O_2 reaction would lead to transfer of one of the two oxygen atoms of molecular oxygen (from a Cu_2O_2-derived reactive species) to a substrate, leaving behind two copper(II) ions (and oxide, hydroxide, or water also derived

(56) Cole, A. P.; Mahadevan, V.; Mirica, L. M.; Ottenwaelder, X.; Stack, T. D. P. *Inorg. Chem.* **2005**, *44*, 7345–7364.
(57) Kajii, Y.; Fujita, M.; Hiratsuka, H.; Obi, K.; Mori, Y.; Tanaka, I. *J. Phys. Chem.* **1987**, *91*, 2791–2794.
(58) Henson, M. J.; Mukherjee, P.; Root, D. E.; Stack, T. D. P.; Solomon, E. I. *J. Am. Chem. Soc.* **1999**, *121*, 10332–10345.
(59) Itoh, S.; Taki, M.; Nakao, H.; Holland, P. L.; Tolman, W. B., Jr.; Fukuzumi, S. *Angew. Chem., Int. Ed.* **2000**, *39*, 398–400.
(60) Itoh, S.; Nakao, H.; Berreau, L. M.; Kondo, T.; Komatsu, M.; Fukuzumi, S. *J. Am. Chem. Soc.* **1998**, *120*, 2890–2899.
(61) Mahapatra, S.; Halfen, J. A.; Tolman, W. B. *J. Am. Chem. Soc.* **1996**, *118*, 11575–11586.
(62) Spuhler, P.; Holthausen, M. C. *Angew. Chem., Int. Ed.* **2003**, *42*, 5961–5965.
(63) Cramer, C. J.; Pak, Y. *Theor. Chem. Acc.* **2001**, *105*, 477–480.

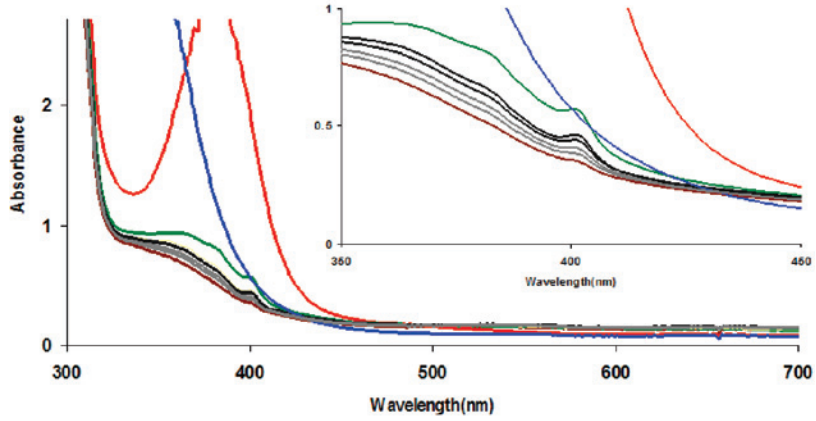

Figure 5. UV–vis spectra at −80 °C in Et_2O, illustrating formation of the **7-O₂** (**red** spectrum) from $[(6tbp)Cu^{I}]^{+}$(**7**) (**blue** spectrum) reaction with dioxygen, followed by addition of 2,4,6-$^{t}Bu_3$-phenol to give a new species (**green** spectrum). The latter decomposes rapidly (within 5 min at −80 °C); the spectra in **black** are observed with time, and these eventually give way to the final (at −80 °C) **brown** spectrum. The inset shows the expanded region containing the 2,4,6-$^{t}Bu_3$ phenoxyl radical at ∼405 nm.

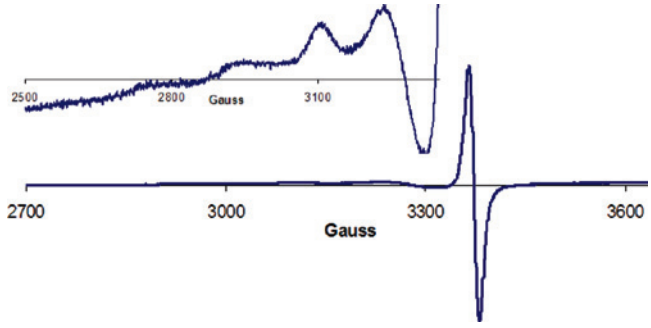

Figure 6. EPR spectrum following reaction of $[\{(6tbp)Cu^{III}\}_2(O^{2-})_2]^{2+}$ (**7-O₂**) with 2,4,6-$^{t}Bu_3$-phenol at 4 K in Et_2O solvent. The products include the 2,4,6-$^{t}Bu_3$-phenoxyl radical (g ≈ 2), along with $[\{(6tbp)_2Cu^{II}Cu^{III}\}(O^{2-})(OH^{-})]^{2+}$ (**7-O₂−H**) or species derived from this {EPR parameters $g_{||} = 2.232$, $A_{||} = 175$ G}, see text.

from O_2).[64,65] Thus the theoretical yield is 50% based on the dicopper center, and thus our observed yields are really 67–70%. For toluene as substrate, a single dicopper(II) product could also be isolated in 85% yield, the bis-μ-hydroxide-bridged complex $[\{(6tbp)Cu^{II}\}_2(^{-}OH)_2]^{2+}$(**7-OH**). Its formulation is supported by IR ($\nu_{OH} = 3580$ cm^{-1})[50] and EPR (silent) spectroscopies along with its elemental analysis (see Experimental Section).

When $^{18}O_2$ was employed to generate $[\{(6tbp)Cu^{III}\}_2(^{18}O^{2-})_2]^{2+}$ (**7-^{18}O₂**) in toluene, workup revealed the formation of PhCH^{18}O, with ∼70% ^{18}O incorporation.[31] Thus, the O-atom in the benzaldehyde product is dioxygen derived. Further insights came from a competitive intermolecular substrate oxidation reaction, where **7-O₂** was generated within a 1:1 solution mixture of $PhCH_3$ and $PhCD_3$. The result was formation of PhCHO and PhCDO in a ∼7:1 ratio, as determined by GC and GC-MS spectrometry. Thus, an apparent deuterium isotope effect (k_H/k_D) of ∼7 is observed. In fact, k_H/k_D values vary from 1 to 25 for a wide variety of substrate/bis(μ-oxo)dicopper(III) reactions.[7,20,59,61,62]

With this information in hand, we can suggest mechanisms of reaction for the **7-O₂** mediated oxygenation of toluene. An initial H-atom abstraction from the benzylic toluene methyl group gives a mixed-valent μ-hydroxo-μ-oxo dicopper species **7-O₂−H;** (Scheme 4), that species discussed above in connection with reactions of **7-O₂** with ArOH substrates. {Note: A mixed-valent (μ-oxo)(μ-hydroxo) dimetal(II,III) species has been previously proposed in the oxidation of a supporting ligand mediated by a bis(μ-oxo)dinickel(III) species.}[66] Accompanying formation of this could be a free benzyl radical; however we see no evidence for this in that no coupled product, bibenzyl, could be detected in the reaction product mixture. Thus, perhaps a benzyl radical rebounds to give a μ-(OCH_2Ph)-μ-OH product **7-OH-OR** (Scheme 4, path A) or this forms directly in the original **7-O₂**/toluene reaction. Continuing along Path A, to account for the final products **7-OH** and PhCHO, another mol equiv of **7-O₂** must react with **7-OH-OR** in a process which seems hard to imagine in detail, but which has been discussed previously.[7,20,25,56,58–61] We should point out that absolutely no benzyl alcohol could be detected as a product, which suggests this compound is not released from **7-OH-OR**, which would leave behind a mono-oxo-bridged dicopper(II) complex.

Another possible reaction pathway can involve the benzyl peroxo radical ($PhCH_2OO^{\bullet}$), formed from the reaction of benzyl radical with molecular O_2. The latter would be present because of the dynamic behavior of **7-O₂** (vide infra) via reformation of an O−O bond, that is, the reverse reaction of the copper(I) complex (**7**) oxygenation process. The species $PhCH_2OO^{\bullet}$ can disproportionate via known alkylperoxo radical chemistry to yield PhCHO and $PhCH_2OH$ in 1:1 ratio.[67–69] However, this is likely not what occurs here because PhCHO is the only observed product in **7-O₂**/toluene reactivity (vide supra). Instead, we suggest the likely course of reaction is a $[(6tbp)Cu^{I}]^{+}$ (**7**) reduction of $PhCH_2OO^{\bullet}$ giving the alkylperoxo species $[(6tbp)Cu^{II}\text{-}OOCH_2Ph]^{+}$;[68,69]

(64) Karlin, K. D.; Zuberbühler, A. D. Formation, Structure and Reactivity of Copper Dioxygen Complexes. In *Bioinorganic Catalysis: Second Edition, Revised and Expanded*; Reedijk, J., Bouwman, E., Ed.; Marcel Dekker, Inc.: New York, 1999; pp 469–534..

(65) Karlin, K. D.; Gultneh, Y.; Hayes, J. C.; Cruse, R. W.; McKown, J. W.; Hutchinson, J. P.; Zubieta, J. *J. Am. Chem. Soc.* **1984**, *106*, 2121–2128.

(66) Cho, J.; Furutachi, H.; Fujinami, S.; Tosha, T.; Ohtsu, H.; Ikeda, O.; Suzuki, A.; Nomura, M.; Uruga, T.; Tanida, H.; Kawai, T.; Tanaka, K.; Kitagawa, T.; Suzuki, M. *Inorg. Chem.* **2006**, *45*, 2873–2885.

Scheme 3

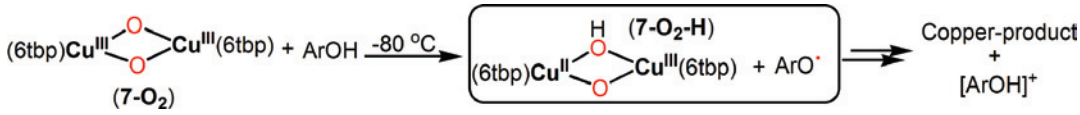

Scheme 4

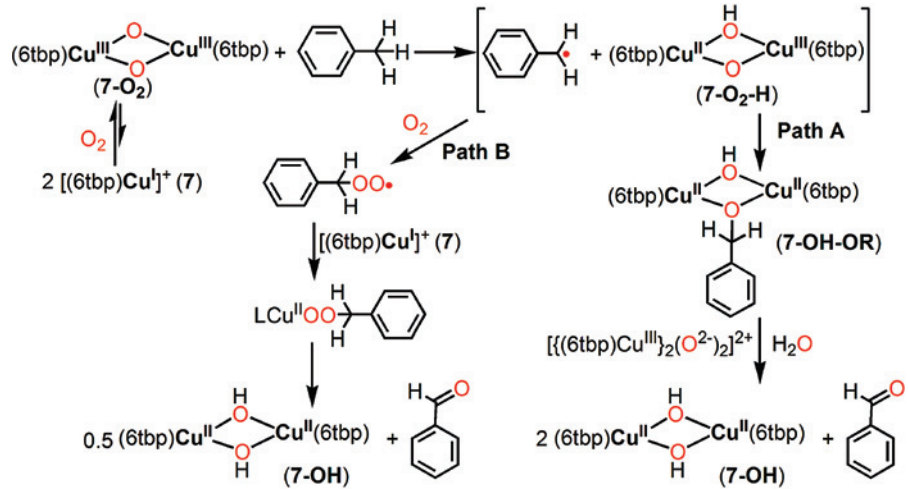

Scheme 5

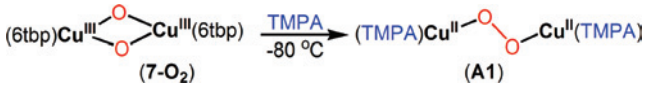

Scheme 6

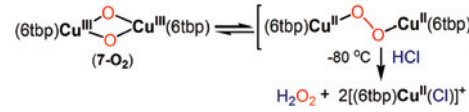

this would then eliminate PhCHO, while concomitantly producing 0.5 equiv of $[\{(6tbp)Cu^{II}\}_2(^{-}OH)_2]^{2+}$ (**7-OH**) (Scheme 4, path B).

Reaction of $[\{(6tbp)Cu^{III}\}_2(O^{2-})_2]^{2+}$ (7-O₂) with TMPA: Ligand Exchange Accompanied by O−O Bond Formation. Evidence for dynamic behavior in the chemistry of **7-O₂** comes from observations of its reactivity with the tripodal tetradentate ligand TMPA. When this (1.1 to excess) is added to solutions of **7-O₂** from which excess O_2 has been removed, $[\{(TMPA)Cu^{II}\}_2(\mu\text{-}1,2\text{-}O_2^{2-})]^{2+}$ (**A1**) forms (Scheme 5). This transformation can be followed spectrophotometrically, Figure 7; a brownish yellow solution of **7-O₂** changes to purple gives the **A1**, with its highly characteristic spectrum. We have previously reported related (di)oxygen transfer reactions.[70]

From the observed spectrum and known absorptivity of $[\{(TMPA)Cu^{II}\}_2(\mu\text{-}1,2\text{-}O_2^{2-})]^{2+}$ (**A1**)[49] in Et_2O solvent,[23,71] one calculates that a 90% conversion of **7-O₂** to **A1** has occurred (Scheme 5). The result indicates a greater overall thermodynamic stability of $[\{(TMPA)Cu^{II}\}_2(\mu\text{-}1,2\text{-}O_2^{2-})]^{2+}$ (**A1**) compared to $[\{(6tbp)Cu^{III}\}_2(O^{2-})_2]^{2+}$ (**7-O₂**). This likely is the result of a lesser ligand electron-donating capability of 6tBP or the steric hindrance coming from the 6-*tert*-butylphenyl substituent which results in Cu−N bond elongation and geometric distortion from trigonal bipyramidal to square pyramidal geometry.[27,28,30,31]

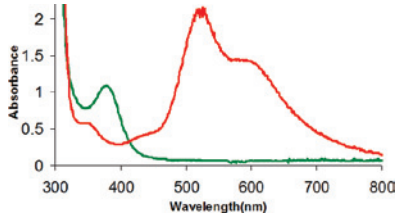

Figure 7. Addition of TMPA to bis(μ-oxo)dicopper(III) complex **7-O₂** at −80 °C in Et_2O (**green** spectrum) leads to immediate formation of $[\{(TMPA)Cu^{II}\}_2(\mu\text{-}1,2\text{-}O_2^{2-})]^{2+}$ (**A1**, **red** spectrum).

Protonation of $[\{(6tbp)Cu^{III}\}_2(O^{2-})_2]^{2+}$ (7-O₂) and Generation of H_2O_2. When a solution of $[\{(6tbp)Cu^{III}\}_2(O^{2-})_2]^{2+}$ (**7-O₂**) in Et_2O at −80 °C is subjected to acid by addition of excess (~2 equiv) dry HCl in Et_2O, an immediate color change to green occurs, and $[\{(6tbp)Cu^{II}(Cl)\}_2]^{2+}$ forms in ~85–90% yield. The identity of this copper(II) product was confirmed by comparison to authentic material (see discussion above and Supporting Information). Hydrogen peroxide is also generated (80% yield); it was identified and quantified using the titanium oxy-sulfate method (see Experimental Section). This result further demonstrates that a reversible equilibrium between bis(μ-oxo)dicopper(III) and (μ-1,2)peroxodicopper(II) complex forms exists. Here, protonation competes favorably with peroxide−Cu(II) binding resulting in the release of H_2O_2 (Scheme 6). We note here that Suzuki and co-workers[10] were even further able to show that O_2 could be released from the bis(μ-oxo)dicopper(III) complex formed using Me_2TPA (Chart 1), either by bubbling solutions with N_2 or by adding PPh_3, the latter which binds strongly to the reformed copper(I) complex.

Summary/Conclusion

We have shown here that subtle steric demands lead to structural changes in ligand-copper(I)/dioxygen complex reactions when the ligand is a tripodal tetradentate analog of TMPA (tris(2-pyridylmethyl)amine) where only one pryidyl arm possesses a 6-substituent. When the 6-pyridyl substituent is a −XHR group (X = N or C), the traditional copper/dioxygen adduct forms, a (μ-1,2)peroxodicopper(II) species (**A**). However, when the substituent is the slightly bulkier XR_2 moiety {aryl or NR_2 ($R \neq H$)}, a bis(μ-oxo)dicopper(III) structure (**C**) is favored (Chart 2).

A −XHR group substitution results in a charge-transfer band energy red shift and decreased $\nu(Cu-O)_s$ stretches compared to those of $[\{(TMPA)Cu^{II}\}_2(\mu\text{-}1,2\text{-}O_2^{2-})]^{2+}$ (**A1**). These changes are ascribed to geometric distortions which lead to decreased overlap between $d_\sigma(Cu)$ and π_σ^* (O_2^{2-}) ligand. There is also an accompanying shift in $\nu(O-O)$ to higher energy, from 830 cm^{-1} for **A1** to 848 cm^{-1} for $[\{(L^{CH_2OMe})Cu^{II}\}_2(\mu\text{-}1,2\text{-}O_2^{2-})]^{2+}$ (**1-O₂**), which could result from mechanical coupling of the Cu−O and O−O modes in a structurally distorted binuclear complex. For the complex $[\{(L^{NH(CH_3)})Cu^{II}\}_2(\mu\text{-}1,2\text{-}O_2^{2-})]^{2+}$ (**2-O₂**), a blue shift of the prominent UV–vis charge-transfer band likely arises from stabilization of the π_σ^* (O_2^{2-}) orbital because of an intramolecular H-bonding interaction, as previously observed by Masuda and co-workers.[39,40] The H-bonding also reduces the lone-pair repulsions of the peroxide, leading to strengthening of the O−O bond with a shift of $\nu(O-O)$ to higher energy (848 cm^{-1}).

The bis(μ-oxo)dicopper(III) species substrate reactivity of our complex $[\{(6tbp)Cu^{III}\}_2(O^{2-})_2]^{2+}$ (**7-O₂**) has been probed, and for the first time (to our knowledge), we can demonstrate exogenous toluene or ethylbenzene hydrocarbon oxygenation. Typical monooxygenase type chemistry results, including ^{18}O-labeling experiments, demonstrate that the oxygen atom in the benzaldehyde product derived from toluene is derived from molecular oxygen. A H-atom abstraction capability in the chemistry of **7-O₂** is apparent from its reactions with ArOH substrates, as well as the determination of $k_H/k_D \approx 7$ in the toluene oxygenation (i.e., demonstrated from competitive reactions with $PhCH_3$ vs $PhCD_3$ substrates). Proposed mechanisms of reaction were presented, including the possible involvement of formation of $PhCH_2OO^\bullet$ and its reaction with copper(I) complex that derives from dynamic solution behavior of **7-O₂**. External TMPA ligand exchange for copper in **7-O₂** and O−O bond (re)formation chemistry, along with the ability to protonate **7-O₂** (which does not possess an O−O bond) and effect release of H_2O_2, indicate an equilibrium between $[\{(6tbp)Cu^{III}\}_2(O^{2-})_2]^{2+}$ (**7-O₂**) and a (μ-1,2)peroxodicopper(II) form.

Acknowledgment. This work was supported by grants from the National Institutes of Health (K.D.K., GM28962; E.I.S, DK31450).

Supporting Information Available: X-ray structure, selected bond lengths and angles, UV–vis, IR, and resonance Raman spectroscopic details, and CIF files. This material is available free of charge on the Internet at http://pubs.acs.org.

IC702437C

(67) Kim, C.; Dong, Y. H.; Que, L. *J. Am. Chem. Soc.* **1997**, *119*, 3635–3636.
(68) Masarwa, A.; Rachmilovich-Calis, S.; Meyerstein, N.; Meyerstein, D. *Coord. Chem. Rev.* **2005**, *249*, 1937–1943.
(69) Goldstein, S.; Meyerstein, D. *Acc. Chem. Res.* **1999**, *32*, 547–550.
(70) Sanyal, I.; Karlin, K. D.; Strange, R. W.; Blackburn, N. J. *J. Am. Chem. Soc.* **1993**, *115*, 11259–11270.
(71) Zhang, C. X.; Kaderli, S.; Costas, M.; Kim, E.-i.; Neuhold, Y.-M.; Karlin, K. D.; Zuberbühler, A. D. *Inorg. Chem.* **2003**, *42*, 1807–1824.